



This is a repository copy of *Human genetics and neuropathology suggest a link between miR-218 and amyotrophic lateral sclerosis pathophysiology*.

White Rose Research Online URL for this paper:
<http://eprints.whiterose.ac.uk/155028/>

Version: Accepted Version

Article:

Reichenstein, I., Eitan, C., Diaz-Garcia, S. et al. (42 more authors) (2019) Human genetics and neuropathology suggest a link between miR-218 and amyotrophic lateral sclerosis pathophysiology. *Science Translational Medicine*, 11 (523). eaav5264. ISSN 1946-6234

<https://doi.org/10.1126/scitranslmed.aav5264>

This is the author's version of the work. It is posted here by permission of the AAAS for personal use, not for redistribution. The definitive version was published in *Science Translational Medicine* on Vol. 11, Issue 523, 18 Dec 2019, DOI: 10.1126/scitranslmed.aav5264.

Reuse

Items deposited in White Rose Research Online are protected by copyright, with all rights reserved unless indicated otherwise. They may be downloaded and/or printed for private study, or other acts as permitted by national copyright laws. The publisher or other rights holders may allow further reproduction and re-use of the full text version. This is indicated by the licence information on the White Rose Research Online record for the item.

Takedown

If you consider content in White Rose Research Online to be in breach of UK law, please notify us by emailing eprints@whiterose.ac.uk including the URL of the record and the reason for the withdrawal request.



eprints@whiterose.ac.uk
<https://eprints.whiterose.ac.uk/>

Title:

Human genetics and neuropathology suggest a link between miR-218 and amyotrophic lateral sclerosis pathophysiology

Authors: Irit Reichenstein^{1†}, Chen Eitan^{1,2†}, Sandra Diaz-Garcia³, Guy Haim¹, Iddo Magen¹, Aviad Siany¹, Mariah L. Hoye⁴, Natali Rivkin¹, Tsviya Olender¹, Beata Toth¹, Revital Ravid¹, Amitai D. Mandelbaum¹, Eran Yanowski¹, Jing Liang¹, Jeffrey K. Rymer⁵, Rivka Levy⁶, Gilad Beck⁷, Elena Ainbinder⁷, Sali M.K. Farhan^{8,9}, Kimberly A. Lennox¹⁰, Nicole M. Bode¹⁰, Mark A. Behlke¹⁰, Thomas Möller¹¹, Smita Saxena¹², Cristiane A. M. Moreno¹³, Giancarlo Costaguta¹⁴, Kristel R. van Eijk^{2,15}, Hemali Phatnani¹⁶, Ammar Al-Chalabi^{2,17,18}, A. Nazli Basak^{2,19}, Leonard H. van den Berg^{2,15}, Orla Hardiman^{2,20}, John E. Landers^{2,21}, Jesus S. Mora^{2,22}, Karen E. Morrison^{2,23}, Pamela J. Shaw^{2,24}, Jan H. Veldink^{2,15}, Samuel L. Pfaff¹⁴, Ofer Yizhar⁶, Christina Gross⁵, Robert H. Brown Jr.²⁵, John M. Ravits³, Matthew B. Harms¹³, Timothy M. Miller⁴ and Eran Hornstein^{1,2*}

Affiliations:

¹Department of Molecular Genetics, Weizmann Institute of Science, Rehovot 7610001, Israel.

²Project MinE ALS Sequencing consortium

³Department of Neurosciences, UC San Diego, La Jolla, CA 92093, USA.

⁴Department of Neurology, Washington University School of Medicine, St. Louis, MO 63110, USA.

⁵Division of Neurology, Cincinnati Children's Hospital Medical Center; Department of Pediatrics, University of Cincinnati College of Medicine, Cincinnati, OH 45229, USA.

⁶Department of Neurobiology, Weizmann Institute of Science, Rehovot 7610001, Israel.

⁷Stem Cell Core and Advanced Cell Technologies Unit, Department of Life Sciences Core Facilities, Weizmann Institute of Science, Rehovot 7610001, Israel.

⁸Analytic and Translational Genetics Unit, Center for Genomic Medicine, Massachusetts General Hospital, Harvard Medical School, Boston, MA 02114, USA.

⁹The Stanley Center for Psychiatric Research, Broad Institute of MIT and Harvard, Cambridge, MA 02142, USA.

¹⁰Integrated DNA Technologies, 1710 Commercial Park Coralville, IA 52241, USA.

¹¹Department of Neurology, School of Medicine, University of Washington, Seattle, WA 98195, USA.

¹²Department of Neurology, Inselspital University Hospital, University of Bern, Freiburgstrasse 16, CH-3010 Bern, Switzerland and the Department for BioMedical Research, University of Bern, Murtenstrasse 40, CH-3008 Bern, Switzerland.

¹³Department of Neurology, Columbia University, New York, NY 10032, USA.

¹⁴Gene Expression Laboratory and the Howard Hughes Medical Institute, Salk Institute for Biological Studies, La Jolla, CA 92037, USA

¹⁵Department of Neurology, UMC Utrecht Brain Center, University Medical Center Utrecht, Utrecht, 3584 CG, The Netherlands.

¹⁶Center for Genomics of Neurodegenerative Disease (CGND) and New York Genome Center (NYGC) ALS Consortium, New York, NY 10013, USA.

¹⁷Maurice Wohl Clinical Neuroscience Institute and United Kingdom Dementia Research Institute, Department of Basic and Clinical Neuroscience, Department of Neurology, King's College London, London SE5 9RX, UK.

¹⁸Department of Neurology, King's College Hospital, London SE5 9RS, UK.

¹⁹Koç University Translational Medicine Research Center, NDAL, Istanbul 34010, Turkey.

²⁰Academic Unit of Neurology, Trinity College Dublin, Trinity Biomedical Sciences Institute and Department of Neurology, Beaumont Hospital, Dublin 2, Republic of Ireland.

²¹Department of Neurology, University of Massachusetts Medical School, Worcester, MA 01605, USA.

²²ALS Unit, Hospital San Rafael, Madrid 28016, Spain.

²³Faculty of Medicine, University of Southampton, Southampton SO17 1BJ, UK.

²⁴Sheffield Institute for Translational Neuroscience (SITraN), University of Sheffield, Sheffield S10 2HQ, UK.

²⁵Department of Neurology, University of Massachusetts Medical School, Worcester, MA 01655, USA.

†These authors contributed equally to the work

*Corresponding author. Tel: +972 89346215; Fax: +972 89342108; E-mail: Eran.hornstein@weizmann.ac.il

One Sentence Summary: Genetics, pathology and molecular studies demonstrate that miR-218 is modulated and might play a role in amyotrophic lateral sclerosis.

Abstract: Motor-neuron specific microRNA-218 (miR-218) has recently received attention because of its roles in mouse development. However, miR-218 relevance to human motor neuron disease was not yet explored. Here, we demonstrate by neuropathology that miR-218 is abundant in healthy human motor neurons. However, in amyotrophic lateral sclerosis (ALS) motor neurons miR-218 is downregulated and its mRNA targets are reciprocally upregulated (de-repressed). We further identify the potassium channel Kv10.1 as a new miR-218 direct target that controls neuronal activity. In addition, we screened thousands of ALS genomes and identified six rare variants in the human miR-218-2 sequence. miR-218 gene variants fail to regulate neuron activity, suggesting the importance of this small endogenous RNA for neuronal robustness. The underlying mechanisms involve inhibition of miR-218 biogenesis and reduced processing by DICER. Therefore, miR-218 activity in motor neurons may be susceptible to failure in human ALS suggesting that miR-218 may be a potential therapeutic target in motor neuron disease.

[Main Text:]

Introduction

microRNA-218 (miR-218) is an endogenous small RNA that is enriched in motor neurons. Its relevance to motor neuron diseases was recently suggested by showing that miR-218 is essential for perinatal neuromuscular survival (1, 2), it is decreased in human amyotrophic lateral sclerosis (ALS) post-mortem spinal cord (3, 4), that cell-free miR-218 can serve as marker for motor neuron loss in a rodent model of ALS (4) and as a neuron-to-astrocyte signal (5). However, miR-218 was not yet studied in human motor neurons and relevance to human ALS is still missing.

ALS is a fatal disease of the human motor neuron system, characterized by the selective degeneration of cortical and ventral spinal motor neurons.

More than two dozen different genes have been associated with ALS in families or via genome-wide association studies. Mutations in these genes explain only a small fraction of the cases (6-9). Thus, ALS genetic variants in SOD1, NEK1, TARDBP or FUS are observed in <1-3% of cases and the fraction of disease explained by the hexanucleotide repeat at the first exon of C9orf72 is <10% (6, 10). ALS-associated genes are ubiquitously expressed and therefore provide limited insight as to why ALS shows motor neuron-selective vulnerability (8, 11).

Differential susceptibilities could be explained by the dysregulated activity of cell-type specific genes, including miRNAs. Indeed, we and others have shown that miRNA dysregulation is involved in ALS (3, 12-18).

In this study, we demonstrate (i) that miR-218 is specifically enriched in human spinal motor neurons and is downregulated in ALS, (ii) that miR-218 orchestrates neuronal activity in a new pathway upstream of Kv10.1 (Kcnh1) voltage-gated potassium channel and (iii) that rare genetic miR-218 variants, identified in patients with ALS, are detrimental to its biogenesis and function, providing a connection from human genetics to motor neuron-specific functions.

Results

miR-218 is highly and specifically expressed in mature human and murine motor neurons

We sought to evaluate the relevance of miR-218 to human motor neuron and its relevance to ALS. First, miRNA in situ hybridization in human tissues depicted motor neuron specific expression pattern of miR-218 in ventral motor neurons throughout the human spinal cord (Fig. 1A). In parallel, we differentiated human inducible pluripotent stem cells (iPSCs) into motor neurons, following a protocol developed by Kiskinis et al. (19). Accordingly, several mRNA markers of motor neuron differentiation were upregulated, namely, Isl1, Hb9 and ChAT. miR-218 expression was upregulated >2000 fold from undifferentiated pluripotent state to human motor neurons (Fig. 1B). We then assessed miR-218 expression in laser capture microdissection motor neurons from lumbar spinal cords of samples where neurological disease was not reported, by revisiting data that was generated in our previous work (3). miR-218 is specifically enriched in control motor neurons relative to surrounding non motor neuron tissue at the ventral horn of the human lumbar spinal cord or relative to proprioceptive neurons at Clarke's column. Furthermore, assessing miR-218 expression in laser capture microdissection-enriched surviving lumbar motor neurons of patients with ALS that suffered from bulbar onset disease, revealed ~2 fold repression relative to control lumbar motor neurons (Fig. 1C and Datafile S1). We further tested another independent set of postmortem tissues with an orthogonal nanoString nCounter miRNA profiler. This RNA study revealed that miR-218 was the most downregulated miRNA in lumbar ventral horns of sporadic ALS (sALS) nervous systems, relative to non-neurodegeneration controls (Fig. 1D and Datafile S2). Reduced miR-218 in ALS may be explained by loss of motor neurons and / or by molecular downregulation in motor neurons that are still present in the ventral

horn. Accordingly, we have performed miR-218 in situ hybridization that revealed reduced numbers of miR-218⁺ cells in ALS patient tissue relative to non-neurodegeneration controls (Fig. 1E and Datafile S1) and a reduction in the densitometric miR-218 in situ hybridization signal in ALS motor neurons (Fig. 1F). Finally, we demonstrated that there is a global upregulation (de-repression) of miR-218-5p targets in human ALS spinal motor neurons by comparing the expression of top 100 predicted miR-218-5p mRNA targets (TargetScan (20)), in laser capture microdissection-enriched surviving motor neurons from lumbar spinal cords of patients with sALS relative to all expressed mRNAs and to the expression in non-neurodegeneration controls (Fig. 1G (21)). Taken together, our results show that miR-218 is a highly sensitive marker of human spinal motor neurons, whose expression rises high in developing human motor neuron and is maintained in the adult. miR-218 expression is reduced in motor neuron disease because of both molecular downregulation and of motor neuron loss and the mRNA targets of miR-218 are reciprocally upregulated. Therefore, miR-218 might serve as marker of motor neuron mass in the human ventral horn in ALS.

miR-218 regulates motor neuron network activity

To study miR-218 function, we moved to rodent models, whereby miR-218 is specifically expressed in mouse motor neurons, without any preference to motor neuron subtypes (Fig. S1 and (1, 2)). We first performed ontology analysis (22) of predicted miR-218 targets (20). This study identified enrichment in biological processes related to potassium ion transmembrane transport (Fig. 2A). Therefore, we tested the hypothesis that miR-218 regulates primary motor neuron gene expression and activity. Dissociated embryonic mouse spinal cords, were enriched for motor neurons via optiprep gradient sedimentation (23) and transduced with lentiviruses encoding miR-218 overexpression (OE) or miR-218 knockdown (KD). Next generation sequencing (NGS) of RNA revealed that predicted miR-218 targets (TargetScan (20)), were significantly down-regulated following OE of miR-218 (Fig. 2B, $p < 0.0001$). Accordingly, enrichment for two miR-218-5p seed-matches was depicted among mRNAs that were down / up regulated following miR-218 OE / KD, respectively (Sylamer study (24), Fig. 2C,D). No signatures were identified for the target set of any other miRNA. Therefore, the vectors used were specifically affecting miR-218 expression or silencing functions. Expression data are available at gene expression Omnibus (GSE136409).

We then monitored intracellular calcium transients in primary rat motor neurons that overexpressed (~8-fold), or knocked-down (~50%) miR-218. Calcium dynamics were monitored on days 12-13 in vitro, using the Ca^{2+} -sensitive dye, Fluo2 HighAff AM, setting the spike threshold for activity as $\Delta F / F > 2$ over baseline (Fig. 2E,F). miR-218 OE increased the frequency of spontaneous calcium bursts by ~70%, compared to cells that were transduced with control viruses, whereas miR-218 KD attenuated neuronal Ca^{2+}

transient by ~80%, relative to control (Fig. 2G,H). Changes in miR-218 expression did not alter motor neuron viability or morphology (Fig. S2). Therefore, miR-218 regulates neuronal activity.

miR-218 regulates neuronal intrinsic excitability

To test if miR-218 is involved in the regulation of active or passive conductance in neurons, we further employed patch-clamp. However, since primary motor neurons displayed an elevated resting membrane potential of $>-50\text{mV}$ in our hands, consistent with a previous study (25), we were forced to use primary rat hippocampal neurons as alternative, a well-established cell type for patch clamp studies, which expresses miR-218, though less than spinal motor neurons (26-28). Current clamp electrophysiological experiments were performed with CNQX (6-cyano-7-nitroquinoxaline-2,3-dione, AMPA/Kainate blocker) and APV (2-amino-5-phosphonopentanoate, NMDA receptor blocker), on culture days 15-21. In response to current injection (300 pA, 500ms) neuronal firing frequency was ~twofold higher with miR-218 OE, relative to miR-218 KD ($17.9\text{ Hz} \pm 1.3$ vs. 9.4 ± 1.9 Hz, $p<0.01$, Fig. S3A,B) and rheobase, the current input required to generate an action potential (500ms -100 to $+500$ pA steps in 20 pA increments), was ~35% lower in miR-218 OE, relative miE-218 KD (157 ± 12 pA vs. 242 ± 19 pA, $p<0.001$, Fig. S3C,D). Mean voltage threshold for triggering the first spike was unchanged between the different conditions (Fig. S3E) and resting membrane potential (RMP) correlated in a bidirectional manner with miR-218 expression (miR-218 OE -58.8 ± 0.7 mV, $n=65$; control, -60.9 ± 0.7 mV, $n=44$; miR-218 KD -63.7 ± 0.7 mV, $n=30$, $p\text{-value}<0.001$, Fig. S3F). Taken together, network and intrinsic activity studies support the hypothesis that miR-218 regulates neuronal excitability, at least in rat hippocampal neurons.

Kv10.1 functions downstream of miR-218 in motor neurons

To gain molecular insight into the mechanisms by which miR-218 regulates network activity, we next focused on a selected set of relevant targets in the context of neuronal activity. This group includes the potassium channels Kv4.2 (Kcnd2) and Kv10.1 (Kcnh1), GABA receptor subunits Gabrb2 and Gabrg1, GABA transporter GAT1 (Slc6a1) and the calcium channel beta subunit Cacnb4. The changes in the expression of the above six targets, in response to miR-218 overexpression, were validated in an independent set of experiments using qPCR on RNA extracted from rat primary motor neurons (Fig. 3A).

Because miR-218 enhances neuronal activity, we hypothesized that relevant mRNA targets potentially encode for proteins acting downstream of miR-218 in inhibiting neuronal activity. Thus, their KD should increase bursting, reminiscent of miR-218 OE, and concomitant KD of both miR-218 and its target may rescue neuronal activity.

We therefore analyzed the frequency of spontaneous calcium transients in primary motor neurons following candidate target KD, with siRNA nanoparticles that exhibited 20%-80% target mRNA KD (Fig. S4). Non-targeting siRNAs were used as control. Knockdown of either Kv10.1 (Kcnh1) or Kv4.2 (Kcnd2) enhanced the frequency of spontaneous calcium transients and was sufficient to rescue neuronal excitation upon miR-218 inhibition (Fig. 3B-D). In addition, we tested the calcium channel Cacnb4 and GABA pathway components Gabrb2, Gabrg1 and GAT1, which did not obey the requirements to be considered as epistatic downstream effectors of miR-218 in the motor neuron system, under our experimental conditions (Fig. 3E-H).

To substantiate the evidence for the relevance of voltage-gated potassium channels, we performed a series of additional studies that collectively increased our confidence in the relevance of Kv10.1 and were not sufficiently supportive of Kv4.2 in this context.

We demonstrated that both Kv10.1 (Kcna10) or Kv4.2 (Kcnd2) mRNAs can be directly targeted by miR-218, by measuring the luminescence of a Renilla reporter, harboring the 3' untranslated region (3'UTR) of either Kv10.1 (Kcna10) or Kv4.2 (Kcnd2). miR-218 silencing was abrogated by mutated miRNA recognition sequences (Fig. 3I and Fig. S5A). We also mined miRNA-mRNA chimera data from AGO2 cross linking and immunoprecipitation study in the mouse cortex (29). This study revealed miR-218 binding to the 3'UTR of Kv10.1, in vivo in the unmanipulated cortex (Fig. 3J). We next transduced primary rat motor neurons with viral vectors that either overexpress or knockdown miR-218 (Fig. 3K). miR-218 expression reciprocally correlated with Kv10.1 protein under miR-218 KD (Fig. 3L, Fig. S6 and Datafile S3), as could be expected from a genuine target. miR-218 OE did not affect Kv10.1 expression, which might be because of the high basal miR-218 expression in motor neurons. Finally, to test if Kv10.1 is upregulated in ALS, along with miR-218 downregulation, we mined human NGS data, which revealed higher Kv10.1 mRNA expression in ALS, in both induced human motor neurons of patients with ALS ((30) Fig. 3M) and in laser capture microdissection-enriched surviving motor neurons from lumbar spinal cords of patients with sporadic ALS (sALS) with rostral onset and caudal progression ((21) Fig. 3N). A parallel analysis of Kv4.2 expression and regulation was not equally supportive and it is therefore less likely to be regulated by miR-218 in

motor neurons and in ALS (Fig. S5B-F and Datafile S4). Therefore, Kv10.1 appear as a relevant miR-218 target in vitro and in vivo and might be relevant also in human ALS.

Rare miR-218 genetic variants are detected in human patients with ALS

To examine the relevance of miR-218 to human disease we screened for rare genetic variations (minor allele frequency <0.01) in the human miR-218-1 (Chr. 4) and miR-218-2 (Chr. 5) genes in ALS and controls cohorts of Project MinE ALS sequencing consortium data (31). We observed 6 unique rare variants in the precursor miR-218-2 (pre-miR-218-2) gene and a single variant (rs371622197) in pre-miR-218-1 (Fig. 4A and table S1) in multi-national cohorts, which were matched geographically and for ancestry (see methods). None of these variants were harbored within the ~22 nucleotides of mature miR-218-5p [miRBase v20 (32)]. Region-based rare variant association testing by the Optimized Sequence Kernel Association Test (SKAT-O) (33) was non-significant (adjusted p value >0.05). However, odds ratio (OR) was 1.93 with 95% confident interval (CI): 0.42-8.96 (Fig. 4B). We then performed an independent replication study on additional cohorts of Genomic Translation for ALS Care (GTAC), the ALS Sequencing Consortium and the New York Genome Center (NYGC) ALS Consortium for rare miR-218-2 variant association.

Rare miR-218-2 variants were enriched in cases ($p = 0.048$ by SKAT-O; OR=3.06, 95% CI: 0.86 - 10.84). Meta-analysis of both discovery and replication cohorts p value was 0.067 by SKAT-O, (34) and a joint analysis p value was 0.0195 (Chi squared with Yate's correction; OR=2.87, 95% CI: 1.11-7.40; Fig. 4B). Therefore, the burden of variants showed nominal association to the trait ($p < 0.05$), although it did not reach genome-wide significance ($p = 5.0 \times 10^{-8}$) with ALS in our study. Finally, we assessed an independent large cohort of 62,784 non-ALS genomes from NHLBI's Trans-Omics for Precision Medicine (TOPMed). This validation effort yielded a joint p value of 0.0002 by

Chi-Square test with Yate's correction with OR=3.02 (95% CI: 1.65 - 5.52), which confirmed the robustness of the findings (Fig. 4B). This modest excess of rare pre-miR-218-2 variants in ALS did not survive genome wide statistical correction. Taken together, individuals harboring miR-218-2 sequence variants have a risk that is almost three times as high to suffer from ALS, relative to the general population.

Rare miR-218 genetic variants disrupt its ability to regulate neuronal excitability

miRNA genes exhibit high evolutionary conservation and sequence mutations may be detrimental to their function. We sought to test the impact of mutated miR-218 on neuronal activity by intracellular calcium transient recording. The variants were aggregated in two main domains, namely in the loop region, that is supposed to bind DGCR8 (35) and in the miRNA 3' terminal, which is cleaved by Drosha (35, 36) and then becomes an important element of recognition by Dicer (37, 38). To test these variants functionally, we created vectors that represent loop and 3' terminal variants. Then, we transduced primary rat motor neurons with the following miR-218-2 vectors: (i) Control vector, (ii) wild-type human miR-218-2 (WT); (iii) the predominant pre-miRNA loop variant (Chr5:168,195,207, V₂); (iv) the most abundant patient variant at the miRNA 3' terminal (Chr5:168,195,174, V₅); (v) a miR-218-2 version, harboring a collection of variants, superimposed from cases (V_{all}); or (vi) a miR-218-2 sequence that we designed to be resistant to Drosha activity, which yields no mature miR-218 (V_{dead}). Wild-type miR-218 increased spontaneous calcium burst frequency as expected, whereas miR-218 with variant sequences failed to upregulate neuronal Ca²⁺ transient frequency (Fig. 4C,D).

Rare miR-218 genetic variants inhibit its biogenesis

We tested the hypothesis that miR-218 variants impair neuronal bursting, through inhibition of biogenesis or creation of abnormal forms of the mature miRNA. We used HEPG2 cells, which do not express the endogenous miR-218 gene, to over express wild-type or mutated forms of primary miR-218 (pri-miR-218). In addition, we co-transfected miR-214-3p mimics, which served as spike-in control for downstream normalization.

We performed small RNA NGS, on RNA extracted from transfected HEPG2 cells (Fig. 5A). miRNAs were the dominant RNAs in the libraries (56%, Fig. 5B), at approximately a million miRNA reads / library and complexity of ~160 different miRNA species (Fig. 5C). The expression of mature miR-218 following transfection was comparable with the most abundant endogenous miRNAs in HepG2 cells (Fig. 5D). miR-218-5p dominated the expression profile, whereas sequences aligned to the loop or to miR-218-3p were less prevalent, as expected (Fig. 5E). Furthermore, the isomiR-218 profile was comparable across different variants (Fig. 5F). The expression of mature miR-218, derived from mutated forms of pri-miR-218, was lower compared to the wild-type form (Fig. 5G). We validated the drop in mature miR-218 expression, when harboring variants, with quantitative real time PCR (Fig. 5H). We also detected the accumulation of pre-miR-218 forms, following transfection with a vector harboring the most abundant variant (V₅; Fig. 5I), a hallmark of failed biogenesis. The inhibition score (3), describing the ratio of DICER substrate (pre-miR-218) to product (mature miR-218), was increased by 3.4 fold for the predominant pre-miRNA loop variant (V₂) and by 3.1 fold for the most abundant variant (V₅), relative to wild-type miR-218, demonstrating inhibition of miR-218 biogenesis

(Fig. 5J). Taken together, mutated miR-218 exhibits impaired biogenesis, providing a conceivable mechanism for insufficient regulation of neuronal activity.

Discussion

miR-218 was recently put in the spotlight for its roles in motor neuron development (1, 2). The link between perinatal death of mice deficient of miR-218 and a potential deleterious effect in adult humans requires further investigations. In the current work, we demonstrated miR-218 relevance to human motor neurons in a systematic effort that explains how miR-218 contributes to a previously unappreciated facet of motor neuron specificity and disease susceptibility. ALS neuropathology establishes miR-218 as marker of human motor neuron mass and well-being that is downregulated in ALS. Accordingly, mRNA targets of miR-218 are upregulated / de-repressed.

We identified rare sequence variants in the miR-218-2 gene that impair miR-218 biogenesis and its ability to regulate motor neuron activity. These sequence variants are relevant for the understanding of motor neuron health and disease. We suggest that miR-218-2 variants are sub-optimal for a Dicer-dependent step of biogenesis, thus reducing mature miR-218 expression and contributing to selective motor neuron vulnerability. Subtle miR-218 downregulation in humans, plausibly contributes to failed homeostasis in adults, potentially because of broad upregulation (de-repression) of dozens of miR-218 targets in human motor neurons. Furthermore, because miR-218 expression is downregulated in motor neurons of sporadic and familial patients with ALS, individuals harboring miR-218 variants suffer two sequential hits to miR-218 expression and function. Therefore, miR-218 is a relevant candidate for genetic screening in additional ALS genetics cohort.

A previously unrecognized pathway downstream of miR-218 controls neuronal activity by regulating the voltage-gated potassium channel, Kv10.1. Altered motor neuron excitability

and ion channel dysfunction have been reported in patients, rodent and ALS iPSC models (39-51) and drugs such as ezogabine (retigabine) (52), or riluzole, which control potassium and sodium channels, respectively, elude to the relevance of therapeutically altering neuronal activity in ALS.

Additionally, increased expression of voltage-gated potassium channel subtypes have been reported in iPSC-derived ALS motor neurons with FUS and SOD1 mutations and targeting potassium currents with 4-Aminopyridine, a potassium channel blocker, recovered neuronal activity patterns in culture (53). These observations resonate with miR-218 activity upstream of voltage gated potassium channel and suggest that aberrant neuronal activity is an important contributing factor at the ALS milieu.

Our study does not rule out that additional targets may play parallel roles in controlling neuron activity downstream of miR-218. miR-218 is a member of an expanding class of miRNAs that regulate neuronal activity in flies (54, 55) and mammals (56-59), including miR-128 (57), miR-101 (28) and miR-324-5p (60). The emerging regulation of neuronal activity by miRNAs depends on their capacity to fine-tune the expression of dosage-sensitive proteins locally, at dendrites, axons and synapses.

miR-218 regulates a myriad of targets designated Target²¹⁸ (1). Our work, along with reported specific targets in astrocytes and neuronal progenitors (2, 5), contribute to deconvoluting the Target²¹⁸ network. Interestingly, Amin et al. recently showed by a patch clamp study in lumbar spinal slices that miR-218 contributes to inhibiting neuronal activity (1). Reconciling this observation with ours requires new conditional miR-218 alleles that will allow uncoupling miR-218 roles in interneuron differentiation (2) and plausibly in establishing interneuron-motor neuron circuitry, from miR-218 roles in adult motor

neurons. Furthermore, developmental loss of miR-218 causes motor neuron death, further complicating the comparison to the moderate KD in the post-mitotic motor neurons.

In summary, motor-neuron enriched miR-218 might serve as a marker of motor neuron mass in the human ventral horn in ALS and miR-218 functions uncovers previously unappreciated facets of motor neuron specificity that may be particularly susceptible to failure in human patients with ALS. Currently, it is not clear if the global miR-218 downregulation in human neuropathology is a consequence of Dicer inhibition (3) and how such a downregulation might impact non-cell autonomous effects of miR-218 (5). Mouse modelling can be beneficial for exploring miR-218 allele genetic interactions with other ALS-associated mutations and the functional implications of the discovered variants in the miR-218-2 gene sequence. Therefore, the study contributes to an emerging view of ALS as a disease with a prominent RNA component and suggests that miR-218 is a potential therapeutic target for motor neuron disease (graphically summarized in Fig. S7).

Materials and Methods

Study design

The overall objective of our study was to investigate the relevance of motor-neuron specific miR-218 to human motor neuron specificity and disease (summary in Fig. S7), by employing molecular, neurogenetics and neuropathology approaches. First, we performed four orthogonal miRNA quantification studies in human motor neurons: (1) chromogenic miR-218 in situ hybridization in human spinal cord, (2) nanoString nCounter, (3) miR-218 qPCR, and (4) analysis of mRNA expression of miR-218 targets from laser capture microdissection-enriched surviving motor neurons from lumbar spinal cords of patients with sALS. These experiments established miR-218 as marker of human motor neuron mass and well-being. To test whether miR-218 regulates motor neuron activity we transduced primary motor neuron with lentiviruses encoding miR-218 OE or KD and monitored intracellular calcium transients and intrinsic activity by patch-clamp electrophysiological experiments. A series of bioinformatics and experimental steps collectively directed us to conclude that Kv10.1 is a direct target of miR-218 in this system. Using statistical genetics and burden studies of rare variants, we identified miR-218 genetic variants in large ALS cohorts. The variants were shown to inhibit biogenesis and to impair miR-218 function. Experimentalists were blinded while analyzing data. Outliers were excluded if deviated ± 2 SDs away from mean. The number of samples that were taken for case-control cohort in neuropathology (Human motor neuron systems: 20 ALS cases, 14 non-neurodegeneration controls) and neurogenetics (Human genomes: 7,738 ALS, 71,656 controls). These numbers reflect the maximal availability at the time of the study.

Statistical analysis

Statistics performed with Prism Origin (GraphPad Software Inc.). Shapiro-Wilk test was used to assess normality of the data. Pair-wise comparisons passing normality test were analyzed with Student's t-test whereas the Mann-Whitney test was used for pairwise comparison of nonparametric data. Multiple group comparisons passing normality test were analyzed using ANOVA with post hoc tests, whereas nonparametric multiple group comparisons were analyzed using the Kruskal-Wallis test with Dunn's post hoc testing, when ANOVA assumptions were not met. Statistical P values <0.05 were considered significant. Data presented as specified in the figure legends. Data are shown as means \pm SEM or SD or graphed using boxplots, as noted in the text. Individual subject level data are reported in Datafile S1.

Supplementary Materials

Materials and Methods

Fig. S1. miR-218 is highly and specifically expressed in human and murine spinal motor neurons.

Fig. S2. High content analysis (HCA) of neuronal morphology following miR-218 perturbation.

Fig. S3. miR-218 regulates intrinsic excitability.

Fig. S4. qPCR validation of miR-218 target knockdown.

Fig. S5. Evaluation of miR-218 upstream of the mRNA encoding for the potassium channel Kv4.2 (Kcnd2).

Fig. S6. Kv10.1 (Kcnh1) protein quantification by western blot, following miR-218 KD.

Fig. S7. A summary diagram of key observations.

Table S1. Identified hsa-miR-218-2 variants.

Table S2. DsiRNA sequences employed in the study.

Table S3. Synthetic miR-218 sequences used for cloning into pMA-T vectors.

Table S4. Primers used for quantitative real-time PCR.

Data File S1. Individual-level data for miR-218 expression.

Data File S2. NanoString nCounter data for miRNAs measured in lumbar ventral horns.

Data File S3. Source data for Kv10.1 (Kcnh1) western blot studies.

Data File S4. Source data for Kv4.2 (Kcnd2) western blot studies.

References (61-72)

References and Notes:

1. N. D. Amin, G. Bai, J. R. Klug, D. Bonanomi, M. T. Pankratz, W. D. Gifford, C. A. Hinckley, M. J. Sternfeld, S. P. Driscoll, B. Dominguez, K. F. Lee, X. Jin, S. L. Pfaff, Loss of motoneuron-specific microRNA-218 causes systemic neuromuscular failure. *Science* **350**, 1525-1529 (2015).
2. K. P. Thiebes, H. Nam, X. A. Cambronne, R. Shen, S. M. Glasgow, H. H. Cho, J. S. Kwon, R. H. Goodman, J. W. Lee, S. Lee, S. K. Lee, miR-218 is essential to establish motor neuron fate as a downstream effector of Isl1-Lhx3. *Nat Commun* **6**, 7718 (2015).
3. A. Emde, C. Eitan, L. L. Liou, R. T. Libby, N. Rivkin, I. Magen, I. Reichenstein, H. Oppenheim, R. Eilam, A. Silvestroni, B. Alajajian, I. Z. Ben-Dov, J. Aebischer, A. Savidor, Y. Levin, R. Sons, S. M. Hammond, J. M. Ravits, T. Moller, E. Hornstein, Dysregulated miRNA biogenesis downstream of cellular stress and ALS-causing mutations: a new mechanism for ALS. *The EMBO journal* **34**, 2633-2651 (2015).
4. M. L. Hoye, E. D. Koval, A. J. Wegener, T. S. Hyman, C. Yang, D. R. O'Brien, R. L. Miller, T. Cole, K. M. Schoch, T. Shen, T. Kunikata, J. P. Richard, D. H. Gutmann, N. J. Maragakis, H. B. Kordasiewicz, J. D. Dougherty, T. M. Miller, MicroRNA Profiling Reveals Marker of Motor Neuron Disease in ALS Models. *J Neurosci* **37**, 5574-5586 (2017).
5. M. L. Hoye, M. R. Regan, L. A. Jensen, A. M. Lake, L. V. Reddy, S. Vidensky, J. P. Richard, N. J. Maragakis, J. D. Rothstein, J. D. Dougherty, T. M. Miller, Motor

- neuron-derived microRNAs cause astrocyte dysfunction in amyotrophic lateral sclerosis. *Brain*, (2018).
6. A. E. Renton, A. Chio, B. J. Traynor, State of play in amyotrophic lateral sclerosis genetics. *Nat Neurosci* **17**, 17-23 (2014).
 7. J. Cady, P. Allred, T. Bali, A. Pestronk, A. Goate, T. M. Miller, R. D. Mitra, J. Ravits, M. B. Harms, R. H. Baloh, Amyotrophic lateral sclerosis onset is influenced by the burden of rare variants in known amyotrophic lateral sclerosis genes. *Ann Neurol* **77**, 100-113 (2015).
 8. R. H. Brown, A. Al-Chalabi, Amyotrophic Lateral Sclerosis. *N Engl J Med* **377**, 162-172 (2017).
 9. A. Al-Chalabi, L. H. van den Berg, J. Veldink, Gene discovery in amyotrophic lateral sclerosis: implications for clinical management. *Nat Rev Neurol* **13**, 96-104 (2017).
 10. K. P. Kenna, P. T. van Doormaal, A. M. Dekker, N. Ticozzi, B. J. Kenna, F. P. Diekstra, W. van Rheenen, K. R. van Eijk, A. R. Jones, P. Keagle, A. Shatunov, W. Sproviero, B. N. Smith, M. A. van Es, S. D. Topp, A. Kenna, J. W. Miller, C. Fallini, C. Tiloca, R. L. McLaughlin, C. Vance, C. Troakes, C. Colombrita, G. Mora, A. Calvo, F. Verde, S. Al-Sarraj, A. King, D. Calini, J. de Bellerocche, F. Baas, A. J. van der Kooi, M. de Visser, A. L. Ten Asbroek, P. C. Sapp, D. McKenna-Yasek, M. Polak, S. Asress, J. L. Munoz-Blanco, T. M. Strom, T. Meitinger, K. E. Morrison, S. Consortium, G. Lauria, K. L. Williams, P. N. Leigh, G. A. Nicholson, I. P. Blair, C. S. Leblond, P. A. Dion, G. A. Rouleau, H. Pall, P. J. Shaw, M. R. Turner, K. Talbot, F. Taroni, K. B. Boylan, M. Van Blitterswijk,

- R. Rademakers, J. Esteban-Perez, A. Garcia-Redondo, P. Van Damme, W. Robberecht, A. Chio, C. Gellera, C. Drepper, M. Sendtner, A. Ratti, J. D. Glass, J. S. Mora, N. A. Basak, O. Hardiman, A. C. Ludolph, P. M. Andersen, J. H. Weishaupt, R. H. Brown, Jr., A. Al-Chalabi, V. Silani, C. E. Shaw, L. H. van den Berg, J. H. Veldink, J. E. Landers, NEK1 variants confer susceptibility to amyotrophic lateral sclerosis. *Nat Genet* **48**, 1037-1042 (2016).
11. J. P. Taylor, R. H. Brown, Jr., D. W. Cleveland, Decoding ALS: from genes to mechanism. *Nature* **539**, 197-206 (2016).
 12. S. Haramati, E. Chapnik, Y. Sztainberg, R. Eilam, R. Zwang, N. Gershoni, E. McGlinn, P. W. Heiser, A. M. Wills, I. Wirguin, L. L. Rubin, H. Misawa, C. J. Tabin, R. Brown, Jr., A. Chen, E. Hornstein, miRNA malfunction causes spinal motor neuron disease. *Proc Natl Acad Sci U S A* **107**, 13111-13116 (2010).
 13. E. D. Koval, C. Shaner, P. Zhang, X. du Maine, K. Fischer, J. Tay, B. N. Chau, G. F. Wu, T. M. Miller, Method for widespread microRNA-155 inhibition prolongs survival in ALS-model mice. *Hum Mol Genet* **22**, 4127-4135 (2013).
 14. E. F. Goodall, P. R. Heath, O. Bandmann, J. Kirby, P. J. Shaw, Neuronal dark matter: the emerging role of microRNAs in neurodegeneration. *Front Cell Neurosci* **7**, 178 (2013).
 15. D. Campos-Melo, C. A. Droppelmann, Z. He, K. Volkening, M. J. Strong, Altered microRNA expression profile in Amyotrophic Lateral Sclerosis: a role in the regulation of NFL mRNA levels. *Mol Brain* **6**, 26 (2013).
 16. C. Eitan, E. Hornstein, Vulnerability of microRNA biogenesis in FTD-ALS. *Brain Res*, (2016).

17. C. Figueroa-Romero, J. Hur, J. S. Lunn, X. Paez-Colasante, D. E. Bender, R. Yung, S. A. Sakowski, E. L. Feldman, Expression of microRNAs in human post-mortem amyotrophic lateral sclerosis spinal cords provides insight into disease mechanisms. *Mol Cell Neurosci* **71**, 34-45 (2016).
18. Y. T. Tung, K. C. Peng, Y. C. Chen, Y. P. Yen, M. Chang, S. Thams, J. A. Chen, Mir-17 approximately 92 Confers Motor Neuron Subtype Differential Resistance to ALS-Associated Degeneration. *Cell Stem Cell*, (2019).
19. E. Kiskinis, J. Sandoe, L. A. Williams, G. L. Boulting, R. Moccia, B. J. Wainger, S. Han, T. Peng, S. Thams, S. Mikkilineni, C. Mellin, F. T. Merkle, B. N. Davis-Dusenbery, M. Ziller, D. Oakley, J. Ichida, S. Di Costanzo, N. Atwater, M. L. Maeder, M. J. Goodwin, J. Nemesh, R. E. Handsaker, D. Paull, S. Noggle, S. A. McCarroll, J. K. Joung, C. J. Woolf, R. H. Brown, K. Eggan, Pathways disrupted in human ALS motor neurons identified through genetic correction of mutant SOD1. *Cell Stem Cell* **14**, 781-795 (2014).
20. V. Agarwal, G. W. Bell, J. W. Nam, D. P. Bartel, Predicting effective microRNA target sites in mammalian mRNAs. *Elife* **4**, (2015).
21. F. Krach, R. Batra, E. C. Wheeler, A. Q. Vu, R. Wang, K. Hutt, S. J. Rabin, M. W. Baughn, R. T. Libby, S. Diaz-Garcia, J. Stauffer, E. Pirie, S. Saberi, M. Rodriguez, A. A. Madrigal, Z. Kohl, B. Winner, G. W. Yeo, J. Ravits, Transcriptome-pathology correlation identifies interplay between TDP-43 and the expression of its kinase CK1E in sporadic ALS. *Acta Neuropathol* **136**, 405-423 (2018).

22. W. Huang da, B. T. Sherman, R. A. Lempicki, Bioinformatics enrichment tools: paths toward the comprehensive functional analysis of large gene lists. *Nucleic Acids Res* **37**, 1-13 (2009).
23. C. Milligan, D. Gifondorwa, Isolation and culture of postnatal spinal motoneurons. *Methods Mol Biol* **793**, 77-85 (2011).
24. S. van Dongen, C. Abreu-Goodger, A. J. Enright, Detecting microRNA binding and siRNA off-target effects from expression data. *Nat Methods* **5**, 1023-1025 (2008).
25. M. Das, P. Molnar, H. Devaraj, M. Poeta, J. J. Hickman, Electrophysiological and morphological characterization of rat embryonic motoneurons in a defined system. *Biotechnol Prog* **19**, 1756-1761 (2003).
26. S. S. Kaalund, M. T. Venø, M. Bak, R. S. Møller, H. Laursen, F. Madsen, H. Broholm, B. Quistorff, P. Uldall, N. Tommerup, S. Kauppinen, A. Sabers, K. Fluiter, L. B. Møller, A. Y. Nossent, A. Silahtaroglu, J. Kjems, E. Aronica, Z. Tümer, Aberrant expression of miR-218 and miR-204 in human mesial temporal lobe epilepsy and hippocampal sclerosis-convergence on axonal guidance. *Epilepsia* **55**, 2017-2027 (2014).
27. G. Siegel, G. Obernosterer, R. Fiore, M. Oehmen, S. Bicker, M. Christensen, S. Khudayberdiev, P. F. Leuschner, C. J. Busch, C. Kane, K. Hubel, F. Dekker, C. Hedberg, B. Rengarajan, C. Drepper, H. Waldmann, S. Kauppinen, M. E. Greenberg, A. Draguhn, M. Rehmsmeier, J. Martinez, G. M. Schratt, A functional screen implicates microRNA-138-dependent regulation of the depalmitoylation

- enzyme APT1 in dendritic spine morphogenesis. *Nat Cell Biol* **11**, 705-716 (2009).
28. G. Lippi, C. C. Fernandes, L. A. Ewell, D. John, B. Romoli, G. Curia, S. R. Taylor, E. P. Frady, A. B. Jensen, J. C. Liu, M. M. Chaabane, C. Belal, J. L. Nathanson, M. Zoli, J. K. Leutgeb, G. Biagini, G. W. Yeo, D. K. Berg, MicroRNA-101 Regulates Multiple Developmental Programs to Constrain Excitation in Adult Neural Networks. *Neuron* **92**, 1337-1351 (2016).
29. M. J. Moore, T. K. Scheel, J. M. Luna, C. Y. Park, J. J. Fak, E. Nishiuchi, C. M. Rice, R. B. Darnell, miRNA-target chimeras reveal miRNA 3'-end pairing as a major determinant of Argonaute target specificity. *Nat Commun* **6**, 8864 (2015).
30. L. Thompson, iMN (Exp 2) - ALS, SMA and Control (unaffected) iMN cell lines differentiated from iPS cell lines using a long differentiation protocol - RNA-seq. (2017).
31. E. A. L. S. S. C. Project Min, Project MinE: study design and pilot analyses of a large-scale whole-genome sequencing study in amyotrophic lateral sclerosis. *Eur J Hum Genet*, (2018).
32. S. Griffiths-Jones, H. K. Saini, S. van Dongen, A. J. Enright, miRBase: tools for microRNA genomics. *Nucleic Acids Res* **36**, D154-158 (2008).
33. S. Lee, M. J. Emond, M. J. Bamshad, K. C. Barnes, M. J. Rieder, D. A. Nickerson, N. G. E. S. P.-E. L. P. Team, D. C. Christiani, M. M. Wurfel, X. Lin, Optimal unified approach for rare-variant association testing with application to small-sample case-control whole-exome sequencing studies. *Am J Hum Genet* **91**, 224-237 (2012).

34. S. Lee, T. M. Teslovich, M. Boehnke, X. Lin, General framework for meta-analysis of rare variants in sequencing association studies. *Am J Hum Genet* **93**, 42-53 (2013).
35. T. A. Nguyen, M. H. Jo, Y. G. Choi, J. Park, S. C. Kwon, S. Hohng, V. N. Kim, J. S. Woo, Functional Anatomy of the Human Microprocessor. *Cell* **161**, 1374-1387 (2015).
36. Y. Lee, C. Ahn, J. Han, H. Choi, J. Kim, J. Yim, J. Lee, P. Provost, O. Radmark, S. Kim, V. N. Kim, The nuclear RNase III Drosha initiates microRNA processing. *Nature* **425**, 415-419 (2003).
37. S. M. Elbashir, W. Lendeckel, T. Tuschl, RNA interference is mediated by 21- and 22-nucleotide RNAs. *Genes Dev* **15**, 188-200 (2001).
38. A. Nykanen, B. Haley, P. D. Zamore, ATP requirements and small interfering RNA structure in the RNA interference pathway. *Cell* **107**, 309-321 (2001).
39. K. Kanai, S. Kuwabara, S. Misawa, N. Tamura, K. Ogawara, M. Nakata, S. Sawai, T. Hattori, H. Bostock, Altered axonal excitability properties in amyotrophic lateral sclerosis: impaired potassium channel function related to disease stage. *Brain* **129**, 953-962 (2006).
40. S. Vucic, G. A. Nicholson, M. C. Kiernan, Cortical hyperexcitability may precede the onset of familial amyotrophic lateral sclerosis. *Brain* **131**, 1540-1550 (2008).
41. J. J. Kuo, T. Siddique, R. Fu, C. J. Heckman, Increased persistent Na(+) current and its effect on excitability in motoneurons cultured from mutant SOD1 mice. *J Physiol* **563**, 843-854 (2005).

42. C. Zona, M. Pieri, I. Carunchio, Voltage-dependent sodium channels in spinal cord motor neurons display rapid recovery from fast inactivation in a mouse model of amyotrophic lateral sclerosis. *J Neurophysiol* **96**, 3314-3322 (2006).
43. C. Bories, J. Amendola, B. Lamotte d'Incamps, J. Durand, Early electrophysiological abnormalities in lumbar motoneurons in a transgenic mouse model of amyotrophic lateral sclerosis. *Eur J Neurosci* **25**, 451-459 (2007).
44. M. Pieri, F. Albo, C. Gaetti, A. Spalloni, C. P. Bengtson, P. Longone, S. Cavalcanti, C. Zona, Altered excitability of motor neurons in a transgenic mouse model of familial amyotrophic lateral sclerosis. *Neurosci Lett* **351**, 153-156 (2003).
45. B. van Zundert, M. H. Peuscher, M. Hynynen, A. Chen, R. L. Neve, R. H. Brown, Jr., M. Constantine-Paton, M. C. Bellingham, Neonatal neuronal circuitry shows hyperexcitable disturbance in a mouse model of the adult-onset neurodegenerative disease amyotrophic lateral sclerosis. *J Neurosci* **28**, 10864-10874 (2008).
46. K. A. Quinlan, J. E. Schuster, R. Fu, T. Siddique, C. J. Heckman, Altered postnatal maturation of electrical properties in spinal motoneurons in a mouse model of amyotrophic lateral sclerosis. *J Physiol* **589**, 2245-2260 (2011).
47. A. Fuchs, S. Kutterer, T. Muhling, J. Duda, B. Schutz, B. Liss, B. U. Keller, J. Roeper, Selective mitochondrial Ca²⁺ uptake deficit in disease endstage vulnerable motoneurons of the SOD1G93A mouse model of amyotrophic lateral sclerosis. *J Physiol* **591**, 2723-2745 (2013).

48. S. Saxena, F. Roselli, K. Singh, K. Leptien, J. P. Julien, F. Gros-Louis, P. Caroni, Neuroprotection through excitability and mTOR required in ALS motoneurons to delay disease and extend survival. *Neuron* **80**, 80-96 (2013).
49. A. C. Devlin, K. Burr, S. Borooah, J. D. Foster, E. M. Cleary, I. Geti, L. Vallier, C. E. Shaw, S. Chandran, G. B. Miles, Human iPSC-derived motoneurons harbouring TARDBP or C9ORF72 ALS mutations are dysfunctional despite maintaining viability. *Nat Commun* **6**, 5999 (2015).
50. Y. Zhang, W. Ni, A. L. Horwich, L. K. Kaczmarek, An ALS-Associated Mutant SOD1 Rapidly Suppresses KCNT1 (Slack) Na⁺-Activated K⁺ Channels in Aplysia Neurons. *J Neurosci* **37**, 2258-2265 (2017).
51. Y. M. Jiang, M. Yamamoto, Y. Kobayashi, T. Yoshihara, Y. Liang, S. Terao, H. Takeuchi, S. Ishigaki, M. Katsuno, H. Adachi, J. Niwa, F. Tanaka, M. Doyu, M. Yoshida, Y. Hashizume, G. Sobue, Gene expression profile of spinal motor neurons in sporadic amyotrophic lateral sclerosis. *Ann Neurol* **57**, 236-251 (2005).
52. B. J. Wainger, E. Kiskinis, C. Mellin, O. Wiskow, S. S. Han, J. Sandoe, N. P. Perez, L. A. Williams, S. Lee, G. Boulting, J. D. Berry, R. H. Brown, Jr., M. E. Cudkowicz, B. P. Bean, K. Eggan, C. J. Woolf, Intrinsic membrane hyperexcitability of amyotrophic lateral sclerosis patient-derived motor neurons. *Cell Rep* **7**, 1-11 (2014).
53. M. Naujock, N. Stanslowsky, S. Bufler, M. Naumann, P. Reinhardt, J. Sternecker, E. Kefalakes, C. Kassebaum, F. Bursch, X. Lojewski, A. Storch, M. Frickenhaus, T. M. Boeckers, S. Putz, M. Demestre, S. Liebau, M. Klingenstein, A. C. Ludolph, R. Dengler, K. S. Kim, A. Hermann, F. Wegner, S. Petri, 4-

- Aminopyridine Induced Activity Rescues Hypoexcitable Motor Neurons from Amyotrophic Lateral Sclerosis Patient-Derived Induced Pluripotent Stem Cells. *Stem Cells* **34**, 1563-1575 (2016).
54. P. Verma, G. J. Augustine, M. R. Ammar, A. Tashiro, S. M. Cohen, A neuroprotective role for microRNA miR-1000 mediated by limiting glutamate excitotoxicity. *Nat Neurosci* **18**, 379-385 (2015).
55. T. Guven-Ozkan, G. U. Busto, S. S. Schutte, I. Cervantes-Sandoval, D. K. O'Dowd, R. L. Davis, MiR-980 Is a Memory Suppressor MicroRNA that Regulates the Autism-Susceptibility Gene A2bp1. *Cell Rep* **14**, 1698-1709 (2016).
56. M. M. Harraz, S. M. Eacker, X. Wang, T. M. Dawson, V. L. Dawson, MicroRNA-223 is neuroprotective by targeting glutamate receptors. *Proc Natl Acad Sci U S A* **109**, 18962-18967 (2012).
57. C. L. Tan, J. L. Plotkin, M. T. Veno, M. von Schimmelmann, P. Feinberg, S. Mann, A. Handler, J. Kjems, D. J. Surmeier, D. O'Carroll, P. Greengard, A. Schaefer, MicroRNA-128 governs neuronal excitability and motor behavior in mice. *Science* **342**, 1254-1258 (2013).
58. A. Sakai, F. Saitow, N. Miyake, K. Miyake, T. Shimada, H. Suzuki, miR-7a alleviates the maintenance of neuropathic pain through regulation of neuronal excitability. *Brain* **136**, 2738-2750 (2013).
59. R. Fiore, M. Rajman, C. Schwale, S. Bicker, A. Antoniou, C. Bruehl, A. Draguhn, G. Schratt, MiR-134-dependent regulation of Pumilio-2 is necessary for homeostatic synaptic depression. *The EMBO journal* **33**, 2231-2246 (2014).

60. C. Gross, X. Yao, T. Engel, D. Tiwari, L. Xing, S. Rowley, S. W. Danielson, K. T. Thomas, E. M. Jimenez-Mateos, L. M. Schroeder, R. Y. Pun, S. C. Danzer, D. C. Henshall, G. J. Bassell, MicroRNA-Mediated Downregulation of the Potassium Channel Kv4.2 Contributes to Seizure Onset. *Cell Rep* **17**, 37-45 (2016).
61. C. Racz, R. Petrovski, C. T. Saunders, I. Chorny, S. Kruglyak, E. H. Margulies, H. Y. Chuang, M. Kallberg, S. A. Kumar, A. Liao, K. M. Little, M. P. Stromberg, S. W. Tanner, Isaac: ultra-fast whole-genome secondary analysis on Illumina sequencing platforms. *Bioinformatics* **29**, 2041-2043 (2013).
62. P. Danecek, A. Auton, G. Abecasis, C. A. Albers, E. Banks, M. A. DePristo, R. E. Handsaker, G. Lunter, G. T. Marth, S. T. Sherry, G. McVean, R. Durbin, G. Genomes Project Analysis, The variant call format and VCFtools. *Bioinformatics* **27**, 2156-2158 (2011).
63. A. Manichaikul, J. C. Mychaleckyj, S. S. Rich, K. Daly, M. Sale, W. M. Chen, Robust relationship inference in genome-wide association studies. *Bioinformatics* **26**, 2867-2873 (2010).
64. R. L. Rungta, H. B. Choi, P. J. Lin, R. W. Ko, D. Ashby, J. Nair, M. Manoharan, P. R. Cullis, B. A. Macvicar, Lipid Nanoparticle Delivery of siRNA to Silence Neuronal Gene Expression in the Brain. *Mol Ther Nucleic Acids* **2**, e136 (2013).
65. G. J. Gage, D. R. Kipke, W. Shain, Whole animal perfusion fixation for rodents. *Journal of visualized experiments : JoVE*, (2012).

66. G. J. Nuovo, In situ detection of precursor and mature microRNAs in paraffin embedded, formalin fixed tissues and cell preparations. *Methods* **44**, 39-46 (2008).
67. J. T. Pena, C. Sohn-Lee, S. H. Rouhanifard, J. Ludwig, M. Hafner, A. Mihailovic, C. Lim, D. Holoch, P. Berninger, M. Zavolan, T. Tuschl, miRNA in situ hybridization in formaldehyde and EDC-fixed tissues. *Nat Methods* **6**, 139-141 (2009).
68. G. Obernosterer, J. Martinez, M. Alenius, Locked nucleic acid-based in situ detection of microRNAs in mouse tissue sections. *Nat Protoc* **2**, 1508-1514 (2007).
69. Y. Lavin, D. Winter, R. Blecher-Gonen, E. David, H. Keren-Shaul, M. Merad, S. Jung, I. Amit, Tissue-resident macrophage enhancer landscapes are shaped by the local microenvironment. *Cell* **159**, 1312-1326 (2014).
70. D. Kim, G. Pertea, C. Trapnell, H. Pimentel, R. Kelley, S. L. Salzberg, TopHat2: accurate alignment of transcriptomes in the presence of insertions, deletions and gene fusions. *Genome Biol* **14**, R36 (2013).
71. S. Anders, P. T. Pyl, W. Huber, HTSeq--a Python framework to work with high-throughput sequencing data. *Bioinformatics* **31**, 166-169 (2015).
72. M. I. Love, W. Huber, S. Anders, Moderated estimation of fold change and dispersion for RNA-seq data with DESeq2. *Genome Biol* **15**, 550 (2014).

Acknowledgments: We gratefully acknowledge the contributions of all participants and the investigators who provided biological samples and data for Project Mine ALS sequencing consortium, the Genomic Translation for ALS Care (GTAC), the ALS Sequencing Consortium, the New York Genome Center (NYGC) ALS Consortium and TOPMed (Trans-Omics for Precision Medicine) of the National Heart, Lung, and Blood Institute (NHLBI, <https://www.nhlbiwgs.org/topmed-banner-authorship>). Samples used in this research were in part obtained from the UK National DNA Bank for MND Research, funded by the MND Association and the Wellcome Trust. We would like to thank people with MND and their families for their participation in this project. We acknowledge sample management undertaken by Biobanking Solutions funded by the Medical Research Council at the Centre for Integrated Genomic Medical Research, University of Manchester. The authors would like to thank Tzofar Hajbi and Osnat Amram for veterinary services and husbandry. We thank Andres Mauricio, Jaramillo Flautero, Igor Ulitsky, Menahem Segal, Bernard Atalli, Avraham Yaron, Uri Asheri, Rotem Tal and Giordano Lippi for insightful comments on the manuscript. We are grateful for Noa Sadeh and Menahem Segal for training in calcium imaging, to Haim Barr, Noga Kozler and Alexander Plotnikov for assistance with automated imaging, Tali Shalit and Zeev Melamed for assistance with bioinformatics, Katayun Cohen-Kashi Malina for assistance with patch clamp and Maria J. Rodriguez for histology. Hornstein lab is supported by friends of Dr. Sydney Brenner. EH is Head of Nella and Leon Benozziyo Center for Neurological Diseases and incumbent of Ira & Gail Mondry Professorial chair. **Project Mine ALS Sequencing Consortium collaborators:** Christopher E Shaw (Maurice Wohl Clinical Neuroscience Institute and United Kingdom Dementia Research Institute, Department of Basic and Clinical

Neuroscience, Department of Neurology, King's College London, London, UK), Philip van Damme and Wim Robberecht (Laboratory of Neurobiology, VIB, Vesalius Research Center and Department of Neurosciences, Experimental Neurology and Department of Neurology, University Hospitals Leuven and Research Institute for Neuroscience and Disease (LIND), KU Leuven - University of Leuven, Leuven, Belgium), Jonathan D Glass (Department of Neurology and Emory ALS Center, Emory University School of Medicine, Atlanta, Georgia, USA), Russell L McLaughlin (Population Genetics Laboratory, Smurfit Institute of Genetics, Trinity College Dublin, Dublin, Republic of Ireland), Jesus S Mora Pardina (ALS Unit, Hospital San Rafael, Madrid, Spain), and Monica Povedano Panadés (Biomedical Network Research Center on Neurodegenerative Diseases (CIBERNED), Institute Carlos III and Functional Unit of Amyotrophic Lateral Sclerosis (UFELA), Service of Neurology, Bellvitge, University Hospitalet de Llobregat, Spain). **Genomic Translation for ALS Care (GTAC) Consortium collaborator:** David Goldstein (Institute for Genomic Medicine, Columbia University Irving Medical Center, New York, NY, USA; supported by a grant from Biogen). **Funding:** The work is funded by Target ALS (118945 To E.H., J.M.R. and S.L.P.), Legacy Heritage Fund, Bruno and Ilse Frick Foundation for Research on ALS, Teva Pharmaceutical Industries Ltd as part of the Israeli National Network of Excellence in Neuroscience (NNE) and Minna-James-Heineman Stiftung through Minerva. The research leading to these results has received funding to E.H. from the European Research Council under the European Union's Seventh Framework Programme (FP7/2007-2013) / ERC grant agreement n° 617351. Israel Science Foundation, the ALS-Therapy Alliance, AFM Telethon (20576 to E.H.), Motor Neuron Disease Association (UK), The Thierry Latran Foundation for ALS research, ERA-Net for

Research Programmes on Rare Diseases (FP7), A. Alfred Taubman through IsrALS, Yeda-Sela, Yeda-CEO, Israel Ministry of Trade and Industry, Y. Leon Benozio Institute for Molecular Medicine, Kekst Family Institute for Medical Genetics, David and Fela Shapell Family Center for Genetic Disorders Research, Crown Human Genome Center, Nathan, Shirley, Philip and Charlene Vener New Scientist Fund, Julius and Ray Charlestein Foundation, Fraida Foundation, Wolfson Family Charitable Trust, Adelis Foundation, MERCK (UK), Maria Halphen, Estates of Fannie Sherr, Lola Asseof, Lilly Fulop. S.M.K.F. is supported by the ALS Canada Tim E. Noël Postdoctoral Fellowship. C.E. and I.M. were supported by scholarship from Teva Pharmaceutical Industries Ltd as part of the Israeli National Network of Excellence in Neuroscience (NNE). Work at C. Gross lab was supported by NIH grant (R01NS092705 to C.G.). Work at T.M Miller lab was supported by grants from Project5 for ALS, Target ALS, the National Institute of Neurological Disorders and Stroke (R01NS078398 to T.M.M.; F31NS092340 to M.L.H. and T.M.M.), the Robert Packard Center for ALS Research, University of Missouri Spinal Cord Injury/Disease Research Program and the Hope Center for Neurological Disorders. Work at M. B. Harms lab is funded by grants from ALS Association and from Biogen. R. H. Brown Jr. was funded by ALS Association, ALS Finding a Cure, Angel Fund, ALS-One, Cellucci Fund and NIH grants (R01 NS104022, R01 NS073873 and NS111990-01 to R.H.B.J.). A.A.C. was supported through the following funding organizations under the aegis of JPND - www.jpnd.eu (United Kingdom, Medical Research Council (MR/L501529/1; MR/R024804/1)) and through the Motor Neurone Disease Association. This study represents independent research part funded by the National Institute for Health Research (NIHR) Biomedical Research Centre at South London and Maudsley NHS

Foundation Trust and King's College London. A.N.B. was supported by Suna and Inan Kirac Foundation. J.E.L. is supported by the National Institute of Health/NINDS (R01 NS073873). H.P. was supported by a grant from the ALS Association. **Author contributions:** I.R. and C.E. led the project; I.R. and C.E. contributed to research conception, design, interpretations and wrote the manuscript with E.H.; C.E., T.O., M.L.H., T.M.M., C.D.A.M.M., M.B.H., R.H.B.J., S.M.K.F. and K.R.V.E. contributed to human genetics analysis of rare miR-218 variants in human patients with ALS; C.E., G.H., I.M. and T.O. performed NGS studies; N.R. performed reporter assays; S.D.G. performed human histology studies; J.K.R. and G.C. performed protein quantification by western blots; J.L., R.L., A.S., R.R., B.T., A.D.M. and E.Y. helped performing research; G.B. and E.A. performed hiPSC experiments; J.M.R. and T.M. provided human autopsy material; M.A.B., N.M.B. and K.A.L. developed siRNA oligos; S.S., O.Y., C.G. and S.L.P. provided reagents and expertise; E.H. conceived and supervised the study and wrote the manuscript. All co-authors provided approval of the manuscript. **Competing interests:** M.A.B., N.M.B. and K.A.L. are employed by Integrated DNA Technologies, Inc (IDT), which manufactures reagents similar to some described in the manuscript; M.A.B. owns equity in DHR, the parent company of IDT; T.M.M. holds licensing agreement with Ionis Pharmaceuticals and with C2N, he is on the Advisory Board of Ionis Pharmaceuticals and Biogen and is consulting to Cytokinetics; T.M.M. and M.L.H. are inventors on patent/patent application (PCT/US2016/019602, now U.S. patent application number 15/553,922) submitted by Washington University that covers methods to detect motor neuron disease using miRNAs and to target motor neuron disease miRNAs; T.M.M. is an inventor on patent/patent application (PCT/US2015/053283, now U.S. patent application

number 15/515,909) submitted by Washington University that covers Tau Kinetic Measurements; T.M.M. is an inventor on patent/patent application (PCT/US2013/031500, now U.S. patent application number 16/298,607 with corresponding national stage applications or issued patents in Australia, Canada, Europe and Japan) that is jointly owned with Ionis Pharmaceuticals that covers Methods for modulating tau expression for reducing neurodegenerative syndromes; T.M.M. is an inventor on patent/patent application (Issue #10,273,474) that is jointly owned with Ionis Pharmaceuticals that covers Methods for Modulating Tau Expression for Reducing Seizure and Modifying a Neurodegenerative Syndrome; T.M.M. is an inventor on patent/patent application (61/547,890) submitted by Washington University that covers Metabolism of SOD1 in the CSF; I.R. and E.H. are inventors on pending patent family PCT/IL2016/050328 entitled “Methods of treating motor neuron diseases”. All other authors declare that they have no competing interests.

Data and materials availability: Gene Expression Omnibus accession number: GSE136409. miR-218-2-5p isotypes counting code: <https://github.com/TsviyaOlender/mir-218>. Human miR-218 precursors (miRBase v20 (32)), are at Chr5:168195173-168195236; Chr4: 20529922-20529986 of human genome build 19 (hg19). Human genetics data is publically available from the sequencing consortia: Project MinE, Genomic Translation for ALS Care (GTAC), ALS Sequencing Consortium, New York Genome Center (NYGC) and NHLBI's Trans-Omics for Precision Medicine (TOPMed). All Other data used for this manuscript are available in the manuscript.

Fig. 1. miR-218 is expressed in the human spinal motor neurons and is downregulated

in human ALS. (A-F) Three orthogonal miRNA quantification studies in human motor neurons from 20 ALS cases and 14 non-neurodegeneration controls: (A) miR-218 chromogenic in situ hybridization depicting broad expression along the cervical, thoracic and lumbar regions of the adult human spinal cord. (B) qPCR analysis of miR-218, Hb9, Isl1 and ChAT in human iPSCs and differentiated motor neurons. miR-218 normalized to U6 expression. mRNAs normalized to average of HPRT and β -actin expression, presented on a log scale; n=3 independent wells per time point. (C) miR-218 expression in laser-capture micro-dissected human lumbar motor neurons. miR-218 expression in non-neurodegeneration motor neurons (n=7 human spinal cords), relative to surrounding non-motor neuron anterior horn tissue (n=10), to Clarke's column proprioceptive neurons (n=4), or to ALS motor neurons (n=9 sporadic and 2 familial nervous systems carrying the SOD1 A4V mutation). TaqMan qPCR analysis of miR-218 normalized to the average of RNU48/SNORD48, RNU44/SNORD44 and U6 in the same sample, and to the average miR-218 expression in the anterior horn. One-way ANOVA followed by Newman-Keuls multiple comparison test performed on log-transformed data, Means \pm SD. (D) Volcano plot of relative miRNA expression in ALS lumbar ventral horns (n=5), versus non-neurodegeneration controls (n=2; x-axis log2 scale), screened by nanoString nCounter platform. y-axis depicts the differential expression p-values (-log10 scale). Black dots indicate P < 0.05; light gray dots are non-significant. miR-218 is the most downregulated miRNA in ALS nervous systems. Data normalized to the average of five control mRNAs (ACTB, B2M,

GAPDH, RPL19, RPLP0). (E) Reduced miR-218⁺ cell numbers in sALS patient anterior horns (n=4), relative to non-neurodegeneration controls (n=5) and representative miRNA in situ hybridization micrographs. Two way ANOVA followed by Bonferroni's multiple comparison test, Means \pm SEM, and (F) chromogenic miR-218 in situ hybridization signal densitometry in motor neurons at different spinal cord levels (non-neurodegeneration control/ALS cases: Cervical n=151/85 cells; Thoracic n=54/75; Lumbar 189/92). One-tailed Mann-Whitney test, Means \pm SEM. (G) Cumulative distribution function (CDF) plot of top 100 predicted miR-218-5p targets (TargetScan (20)), or all expressed mRNAs, in laser capture microdissection-enriched surviving motor neurons from lumbar spinal cords of patients with sALS with rostral onset and caudal progression (n=13) relative to non-neurodegeneration controls (n=6; (21)) and Box-Plot (inset) depicting median, upper and lower quartiles and extreme points. P-value calculated using Kolmogorov–Smirnov test comparing miR-218-5p targets subset distribution to all genes. * P<0.05; *** P<0.001; **** P<0.0001.

Fig. 2. miR-218 controls motor neuron network activity. (A) Seven most enriched gene ontology terms (22) of predicted miR-218 targets (20). p-value of term enrichment ($-\log_{10}$, dashed orange line indicates $P = 0.05$). (B) CDF plot of miR-218 predicted targets, relative to all expressed mRNAs, following OE of miR-218 and box-plot (insets), depicting median, upper and lower quartiles and extreme points. P-value calculated using Kolmogorov–Smirnov test comparing miR-218-5p subset distribution to all genes. **** $P < 0.0001$. Binding site enrichment of all known miRNAs, in ~10,000 expressed mRNAs, was tested after (C) miR-218 OE, or (D) miR-218 KD, relative to control virus. Significant enrichment for two miR-218-5p seed-matches (blue, red) and lack of enrichment for any other miRNA (gray) via a Sylamer study (24). (E) Diagram of calcium transient imaging in embryonic rat spinal motor neurons, transduced with lentiviruses encoding control vector, miR-218 OE or a miR-218 KD. Neuron time lapse micrographs (F), representative traces (G) and (H) quantification of spontaneous calcium spike frequencies ($\Delta F/F > 0.5$) from Fluo2 HighAff AM study after 12 days in vitro. Recorded from 58 / 76 / 41 control / OE / KD cells, respectively. Box-Plot depicting the median, upper and lower quartiles and extreme points. Kruskal-Wallis test followed by Dunn's multiple comparison test, *** $P < 0.001$. This experiment was repeated 3 independent times with similar results.

Fig. 3. The potassium channel Kv10.1 acts downstream of miR-218. (A) qPCR measuring the expression of mRNAs targets, following miR-218 OE (n=15). Data normalized to control virus (n=12) and to average expression of HPRT and β -actin, two technical duplicates, two-sided student's t-test, Means \pm SEM. (B) Representative traces of individual motor neurons and (C-H) quantification of spontaneous calcium spike frequencies ($\Delta F/F > 0.5$) of embryonic rat spinal motor neurons, transduced with lentiviruses encoding a control vector or miR-218 KD and further transfected with siRNA for specific target KD or a non-targeting siRNA control (minus sign). ≥ 55 cells recorded per each experimental condition; $N \geq 2$ independent experimental repeats with similar results. Kruskal-Wallis test followed by Dunn's multiple comparison test. (I) Relative Renilla luminescence upstream of a wild-type Kv10.1 3'UTR or a mutated 3'UTR that is insensitive to miR-218, normalized to co-expressed firefly luciferase and to a negative control miRNA vector. n=3 independent wells per experimental condition. One-way ANOVA followed by Bonferroni's multiple comparison test. Means \pm SEM. (J) miR-218:Kv10.1 3'UTR chimera from an AGO2 CLEAR-CLIP experiment in mouse cortex (29). (K) miR-218 expression (qPCR n=3, normalized to U6) and (L) Kv10.1 protein expression (Western blot n=5), upon miR-218 lentiviral KD or OE, in primary rat motor neurons and a representative blot detected with anti Kv10.1 and anti Tubulin Beta-III (TUBB3) antibodies. Box-Plots depict median, upper / lower quartiles & extreme points, one-way ANOVA followed by Newman-Keuls multiple comparison test. (M) Kv10.1 mRNA expression, as log₂ normalized counts, from NGS study of induced ALS motor neurons (n=4 different donors in

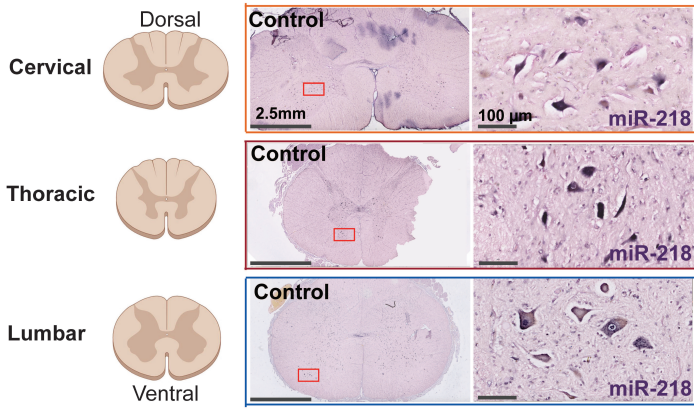
duplicates) or non-neurodegeneration controls (n=3 different donors in duplicates; (30)). Box-Plots depict median, upper / lower quartiles & extreme points, DESeq analysis. (N) Kv10.1 mRNA expression, as Reads Per Kilobase Million (RPKM) from NGS study of laser capture microdissection-enriched surviving motor neurons from lumbar spinal cords of patients with sALS with rostral onset and caudal progression (n=12) and non-neurodegeneration controls (n=8; (21), GSE76220). Box-Plots depict median, upper / lower quartiles & extreme points, two-sided student's t-test. * P<0.05; ** P<0.01; *** P<0.001; ns – non-significant.

Fig. 4. Rare genetic miR-218 variants disrupt its ability to regulate neuronal activity.

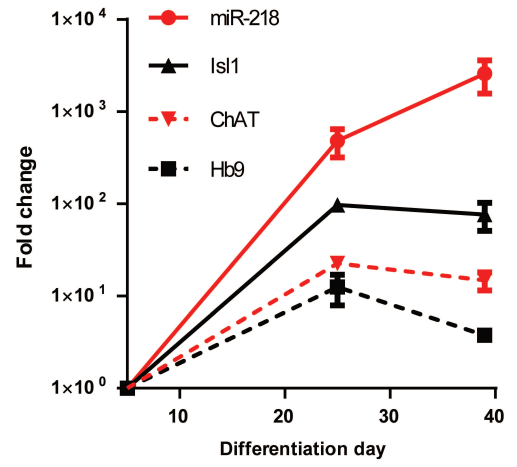
(A) Diagrams of miR-218-2 pri-miRNA (upper) and the pre-miRNA hairpin (lower), with demarcation of DROSHA, DGCR8 and DICER binding and arrows, revealing variant nucleotides (V1-V6). Guide RNA in red. (B) Table and forest plot depicting odds ratio (OR) estimates with 95% confidence intervals (CI), across study cohorts and p-values, calculated with SKAT-O or Chi-squared test with Yate's correction. Vertical dotted line denotes OR=3. (C) Representative motor neuron traces and (D) quantification of spontaneous calcium spike frequencies ($\Delta F/F > 0.5$) in embryonic rat spinal motor neurons, transduced with lentiviruses encoding WT or mutated human miR-218-2. Number of cells recorded in a single experiment: Control, n=131; WT miR-218-2, n=114; single variant V₂, n=137; single variant V₅, n=119; multiple variant V_{all}, n=118; Unprocessable miR-218-2 V_{dead}, n=111. N=4 independent times with similar results. Kruskal-Wallis test followed by Dunn's multiple comparison test. *** P<0.001; ns – non-significant.

Fig. 5. Rare genetic variants in miR-218 inhibit biogenesis. (A) Diagram of experimental design. HEPG2 cells transfected with WT miR-218-2 or miR-218-2 genetic variants and processing of RNA for NGS and qPCR studies. (B) Pie chart of relative representation of different RNA families in NGS data (percentage of reads aligned to miRNA- 56%; tRNA -20%; rRNA – 13%; other RNA types – 11%). (C) The number of expressed miRNAs was comparable across samples. Means \pm SEM. (D) MA plot of miRNA expression in HEPG2 cells transfected with wild-type miR-218-2, relative to control vector. Abundance (x-axis; presented on a log scale) against ratio of miRNA in cells overexpressing WT miR-218 vs a control vector (log₂ fold change). (E) Histogram of number of reads-per-base for WT miR-218-2 sequences, aligned over the genomic sequence. (F) Bar graph of miR-218-2-5p isotypes (isomiR-218-2-5p, sequence denoted) in HEPG2 transfected with WT miR-218-2, or V₂ / V₅ variants. Relative expression of mature miR-218-2 from (G) NGS or (H) TaqMan qPCR studies, normalized to miR-214-3p spike-in mimics. (I) Pre-miR-218-2 expression from NGS. (J) The ratio of pre-miR-218-2 (substrate) to mature miR-218 (product), defined as “inhibition score”. Inhibition score approximates a value of 1 in the WT condition, whereas a value > 1, reflects reduced DICER activity. Control, n=3; WT miR-218-2, n=5; single variant V₂, n=4; single variant V₅, n=4; multiple variant V_{all}, n=5; Unprocessable miR-218-2; V_{dead}, n=3. Box-Plots depict median, upper / lower quartiles & extreme points, One-way ANOVA followed by Bonferroni’s multiple comparison test performed on data (I) or log-transformed data (G, H, J), * P<0.05; ** P<0.01; *** P<0.001; ns – non-significant.

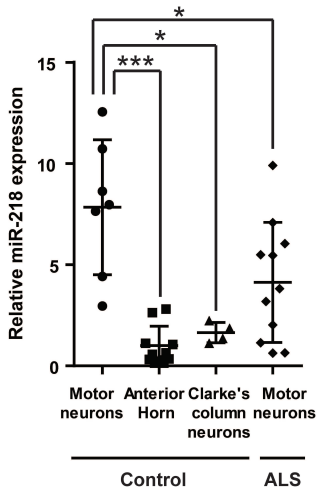
A



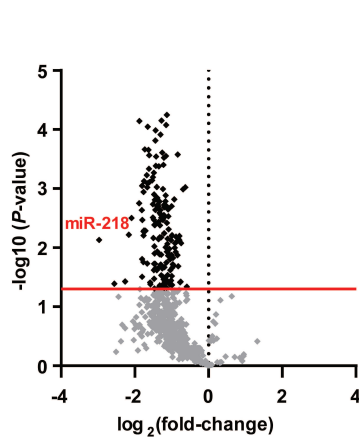
B



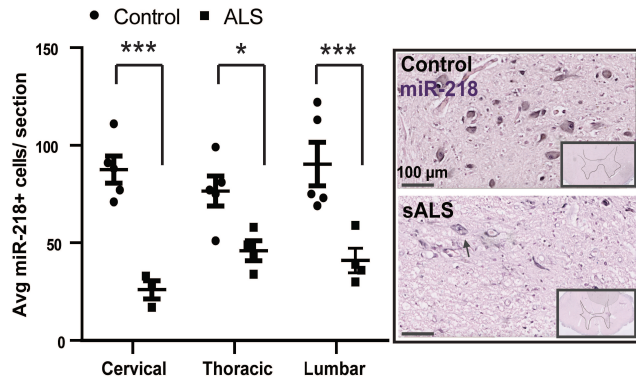
C



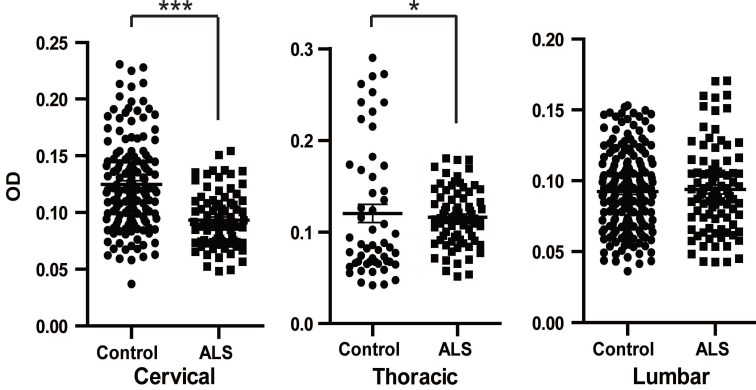
D



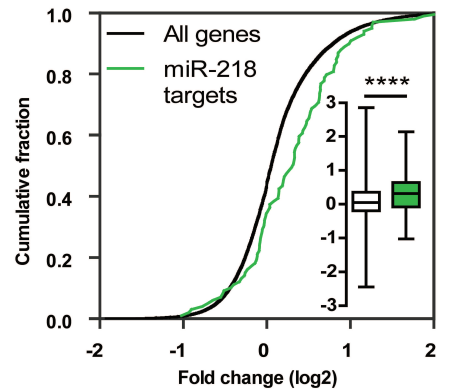
E

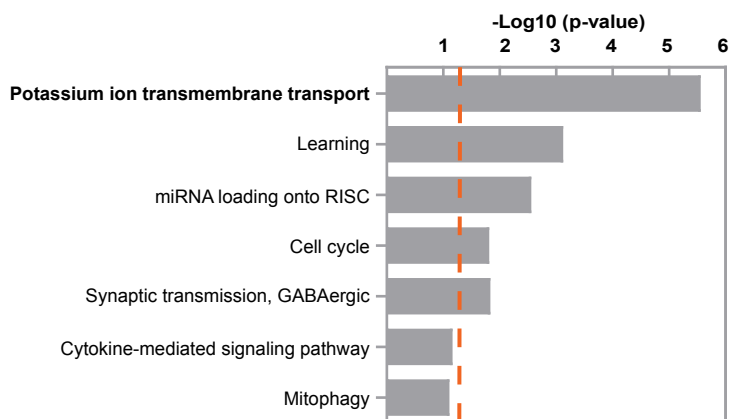
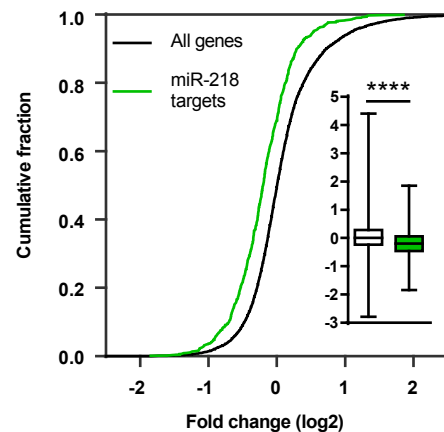
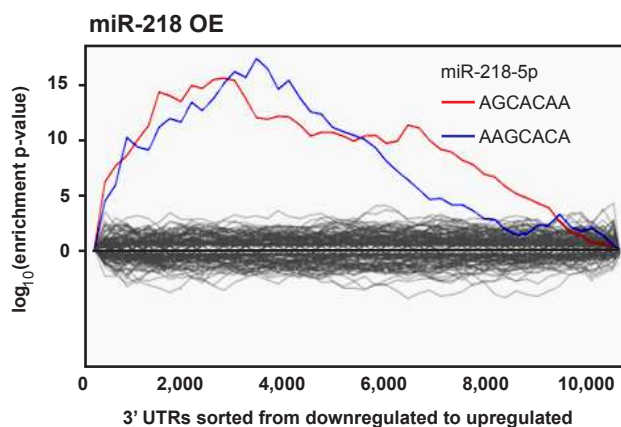
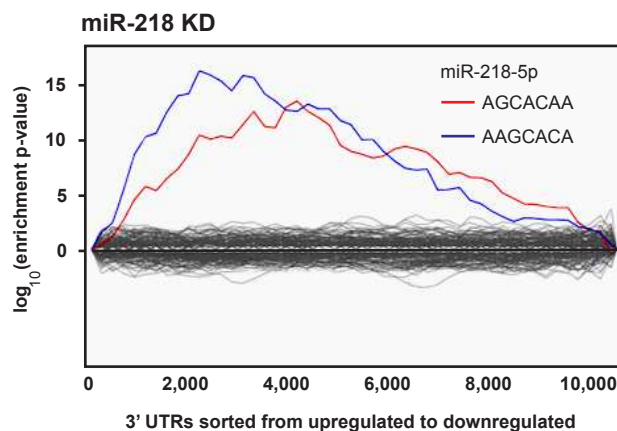
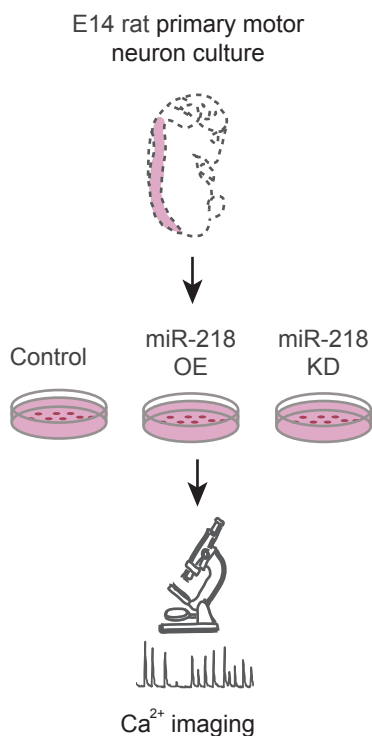
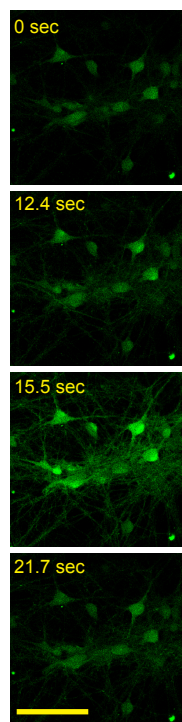
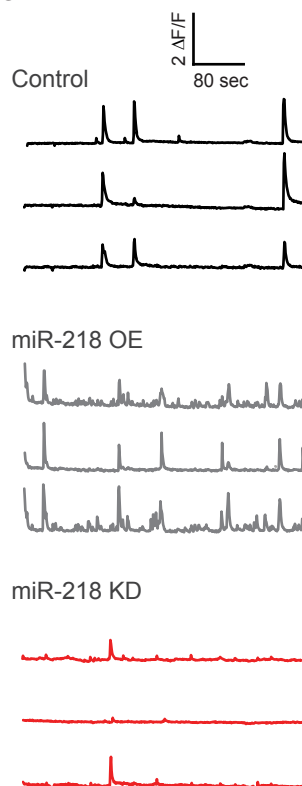
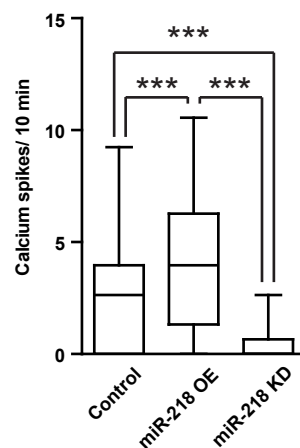


F

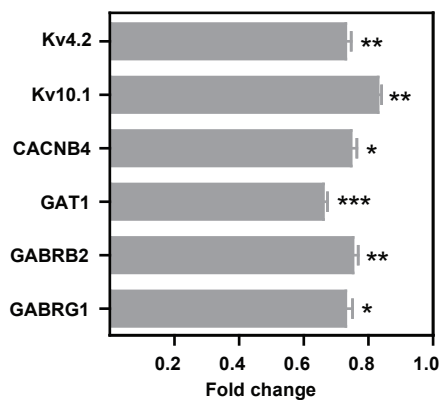


G

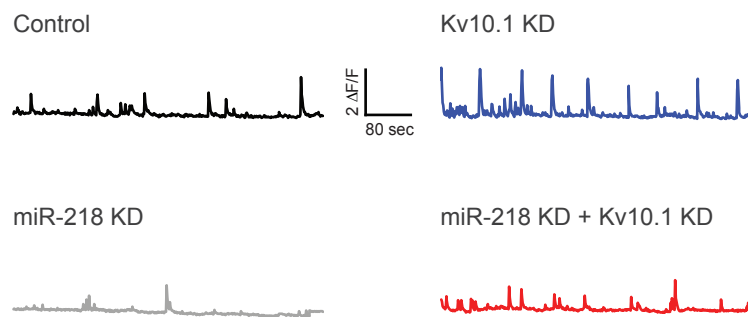


A**B****C****D****E****F****G****H**

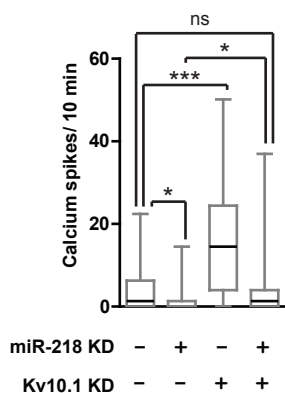
A



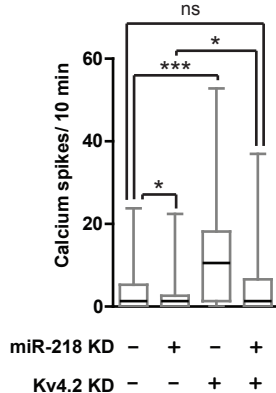
B



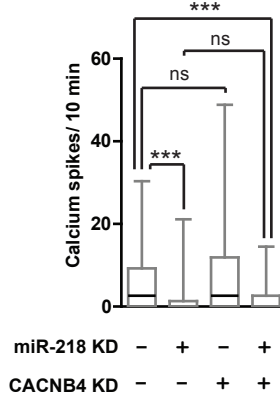
C



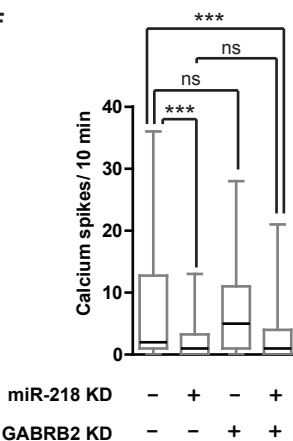
D



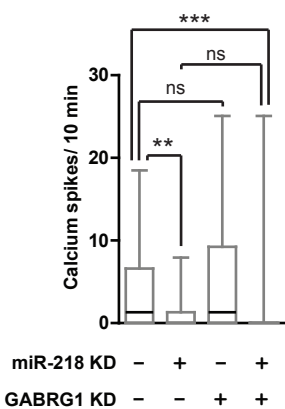
E



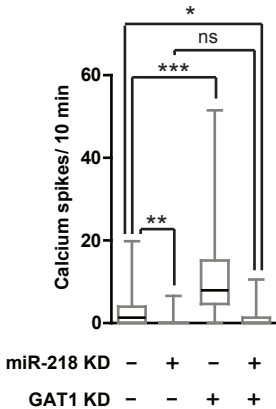
F



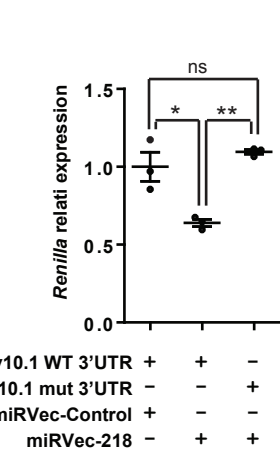
G



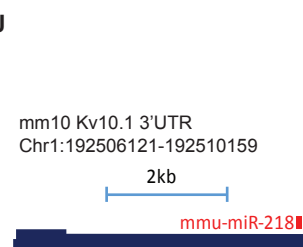
H



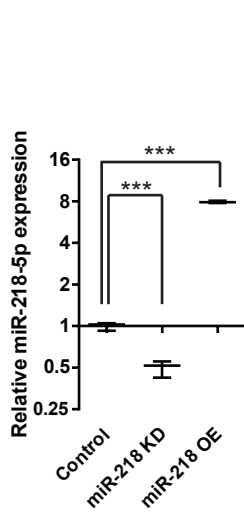
I



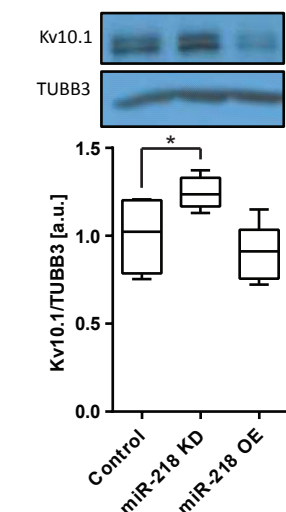
J



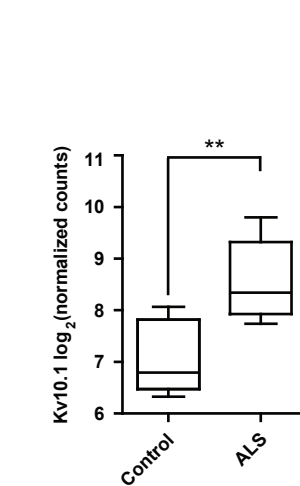
K



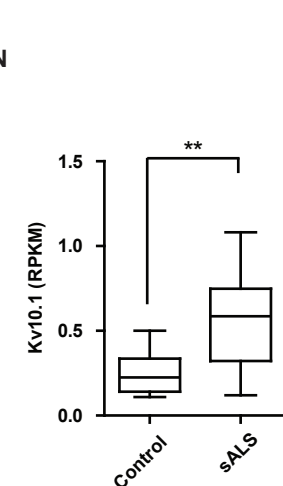
L

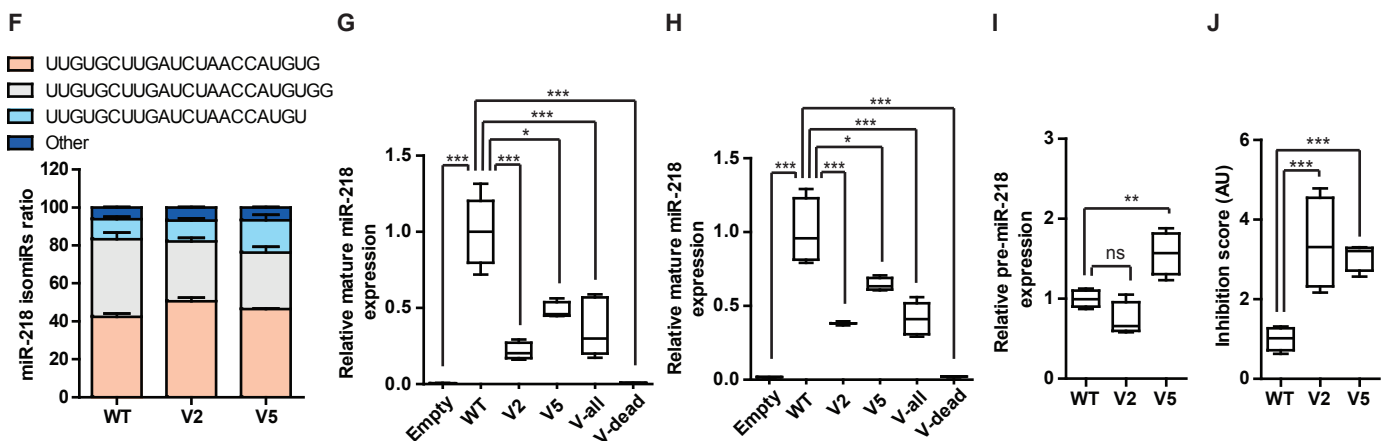
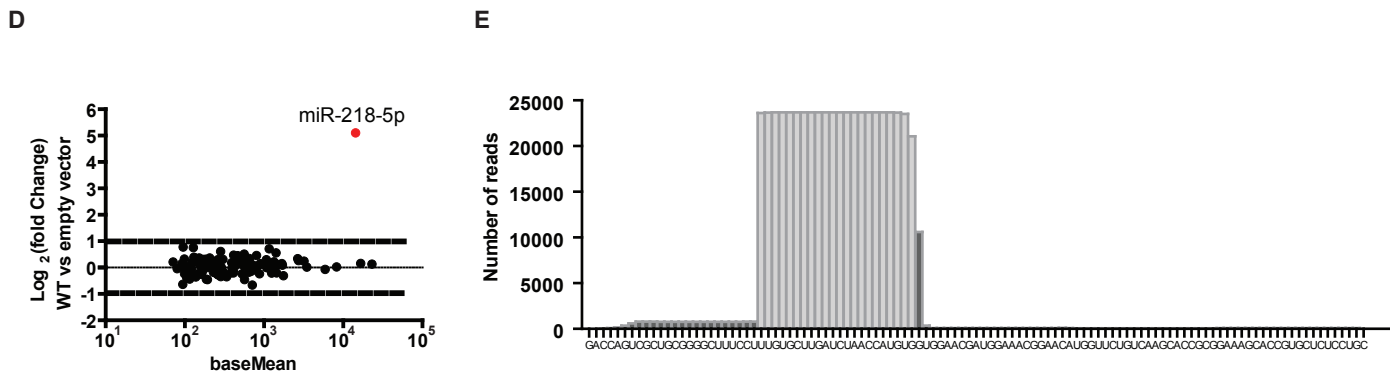
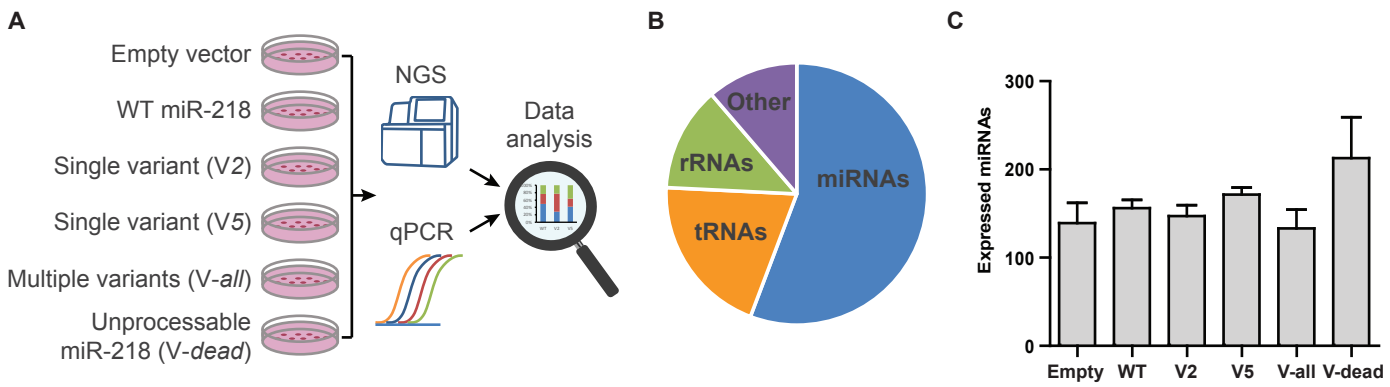


M



N





Materials and Methods

Ethical approval of studies

All subjects contributed DNA for genetic studies approved by local IRBs at the submitting sites. Human materials were studied under approval of Institutional review boards at U.C. San Diego and Weizmann Institute of Science Institutional Review Board. miRNA analysis was performed as previously described (3). All animal experiments were approved by Weizmann Institute of Science IACUC (protocols 33230117-2; 24390116-2; 32271216-1; 23690116-1; 23660116-2; 07201113-1; 02170413-2; 07811212-2).

Human genetics

Project MinE ALS sequencing consortium (31), comprises of seven independent cohorts: the Netherlands, Belgium, Ireland, Spain, United Kingdom, United States and Turkey, served as a discovery cohort. Whole-genome sequencing (WGS) of 6,579 samples was performed on Illumina HiSeq2000 or HiSeqX platforms. Reads were aligned to human genome build hg19 and sequence variants called with Isaac Genome Alignment Software and variant caller (61). Individual genomic variant call format files (GVCFs) were merged with 'agg' tool: a utility for aggregating Illumina-style GVCFs. Multi-allelic variants were excluded from analyses. Following completion of the raw data merge, multiple quality control (QC) filtering steps were performed: (i) setting genotypes with $GQ < 10$ to missing; (ii) removing low-quality sites ($QUAL < 30$ and $QUAL < 20$ for SNPs and indels, respectively); (iii) removing sites with missingness $> 10\%$. (iv) Samples excluded if deviated from mean by more than 6SD for total numbers of SNPs, singletons and indels, Ti/Tv ratio, het/hom-non-ref ratio and inbreeding (by cohort). (v) missingness $> 5\%$, (vi) genotyping-sequence concordance (made possible by genotyping data generated on the

Illumina Omni 2.5M SNP array for all samples; 96% concordance), (vii) depth of coverage, (viii) a gender check (to identify mismatches), (ix) relatedness (drop samples with >100 relatedness pairs). Related individuals were further excluded until no pair of samples had a kinship coefficient > 0.05). (x) missing phenotype information. A total of 6119 samples (4281 ALS cases and 1838 healthy controls) passed all QC and were included in downstream analysis. Per-nucleotide site QC was performed on QC-passing samples only, for biallelic sites: variants were excluded from analysis based on depth (total DP < 10,000 or > 226,000), missingness > 5%, passing rate in the whole dataset < 70%, sites out of Hardy–Weinberg equilibrium (HWE; by cohort, controls only, $p < 1 \times 10^{-6}$) and sites with extreme differential missingness between cases and control samples (overall and by cohort, $p < 1 \times 10^{-6}$). Depth of coverage for all miR-218 variants was >25x.

BED file containing genomic coordinates for miR-218-1,2 precursors (according to miRBase v20 (32)) on human genome build 19 (hg19), Chr5:168195173-168195236; Chr4: 20529922-20529986, was created and variants in these regions were then extracted from the whole-genome sequencing data using vcftools (62). A replication study comprised of data from the Genomic Translation for ALS Care (GTAC), the ALS Sequencing Consortium and the New York Genome Center (NYGC) ALS Consortium genomes and exomes from ALS cases (5336) and non-ALS controls (21388). QC filtering steps were: (i) setting genotypes with GQ<10 to missing; (ii) removing low-quality sites (QUAL) < 30 for SNPs; (iii) removing sites with missingness > 10%; (iv) depth of coverage >10x with >85% of bases in the miR-218-2; (v) a gender check (to identify mismatches); (vi) related individuals by kinship (3 degrees); (vii) missing phenotype information; (viii) ancestry harmonization with iterative EIGENSTRAT cycles. Samples excluded if deviated from

mean by more than 1SD for the first 4 principal components. Finally, 22 samples overlapping with Project Mine dataset were excluded by KING (63). A total of 10,491 samples (3457 ALS cases and 7034 healthy controls) passed all QC. Pass filter rare biallelic variants were included for downstream analyses, tested for Hardy–Weinberg equilibrium and for extreme differential missingness between cases and control samples (overall $p < 1 \times 10^{-6}$).

To further increase sample size, as part of a validation effort, we harvested rare biallelic miR-218-2 variants from 62,784 non-ALS genomes that were available to us through NHLBI's Trans-Omics for Precision Medicine (TOPMed) program.

Association of rare variants, in cases versus controls, in pre-miR-218 genomic region, was evaluated by SKAT-O using 'SKAT' R package (33) with sex and the top 10 PCs as covariates for Project MinE discovery cohort and with sex, platform and the top 3 PCs for replication study. Summary statistics from each study cohort was used to carry out region-based rare variant meta-analysis, by SKAT-O using 'MetaSKAT' R package (34).

TOPMed covariates information is not available, therefore, joint analysis was used, by one tailed Chi square test with Yate's correction, instead of a meta-analysis. We considered a variant to be rare if the minor allele frequency (MAF) < 0.01 .

Immortalized cell lines and transfection

Human embryonic kidney 293T (HEK293T) and HEPG2 cell lines were maintained in Dulbecco's modified Eagle's Medium (DMEM) supplemented with 10% FBS, 1% L-glutamine and 1% Penicillin-streptomycin (Biological industries) at 37 °C with 5% CO₂ incubation. Cells were seeded onto 24-well plates (Corning) 24 h prior to transfection,

in antibiotic- free media and transfected at 70–80% confluence, using Lipofectamine 2000 (Life Technologies) with 800 ng plasmid DNA per 1/24-well plate. For small RNA next generation sequencing (NGS), cells were co-transfected using 1 nM miR-214-3p microRNA mimic (Integrated DNA Technologies, Inc., table S2). Each well was considered as a single technical replicate.

Neuronal cultures

C2 hiPSCs were kindly provided by Dr. Jacob Hanna (Weizmann Institute of Science), cultured and differentiated as previously described (19). Mixed populations of motor neurons were gained, with moderate (30-50% motor neuron enrichment). Primary motor neurons were isolated and cultured as previously described (23). Briefly, Sprague-Dawley timed-pregnant females were sacrificed at rat embryonic day 14.5 (E14.5), and spinal cords were dissected and dissociated enzymatically with papain (2mg/ml, Sigma). Motor neurons were separated over a gradient of Optiprep (Sigma) and plated on 13mm coverslips (200,000 cells/ coverslip, Thermo scientific), pre-coated with 3µg/ml poly-ornithine (Sigma) and 3µg/ml laminin (Gibco). Motor neurons were cultured with Neurobasal medium (Gibco) supplemented with 2% B27 (Gibco) 2% horse serum (Sigma), X1 Glutamax (Gibco) and 1ng/ml CNTF and GDNF (Peprotech). To inhibit glial overgrowth, 200 µM fluorodeoxyuridine (Sigma) was added after 5 days of in vitro culture (DIV). For RNAseq analysis, primary motor neurons were isolated from time pregnant C57BL/6 mice at embryonic day 13.5 (E13.5). Primary cultured hippocampal neurons were prepared from male and female P0 Sprague-Dawley rat pups (Envigo). CA1 and CA3 were isolated, digested with 0.4 mg ml⁻¹ papain (Worthington) and plated onto glass coverslips percolated with 1:30 Matrigel (Corning). Cultured neurons were maintained in a 5%

CO₂ humidified incubator with Neurobasal A medium (Invitrogen) containing 1.25% FBS (Biological Industries), 4% B-27 supplement (Gibco) and 2 mM Glutamax (Gibco) and plated on coverslips in a 24-well plate at a density of 65,000 cells per well. To inhibit glial overgrowth, 200 μ M fluorodeoxyuridine (Sigma) was added after 5 DIV. siRNAs were designed as either single chemically modified 2'OMe DsiRNA molecules, or as pools of 20 unmodified DsiRNA molecules (Integrated DNA Technologies, Inc., table S2). Non-targeting scramble DsiRNAs were used as control (NC5). siRNAs were encapsulated in Neuro9 nanoparticles (Precision NanoSystems, Inc.) (64). Primary motor neurons were transfected with siRNA at a final concentration of 1 μ g/ml, on 9 DIV. Sequences are listed in table S2.

Whole-cell patch clamp recordings

Recordings were performed under QImaging QIClick-R-F-M-12 CCD camera in a chamber perfused with Tyrode's medium (150 mM NaCl, 4 mM KCl, 2 mM MgCl₂, 2 mM CaCl₂, 10 mM D-glucose, 10 mM HEPES; 320 mOsm; pH 7.35; 29 °C) at 0.5 ml / min. Pulled borosilicate glass pipettes (Sutter Instrument BF100-58-10) with resistances 3–5 M Ω , were filled with standard intracellular current clamp recording solution (135 mM potassium gluconate, 4 mM KCl, 2 mM NaCl, 10 mM HEPES, 4 mM EGTA, 4 mM Mg-ATP, 0.3 mM Na-GTP; 280 mOsm; pH 7.3). Recordings were performed using a MultiClamp 700B amplifier, filtered at 3 kHz and digitized at 10 kHz using a Digidata 1440A digitizer (Molecular Devices). Data acquired with pClamp 10 software (Molecular Devices) and analyzed with Matlab (Mathworks). Current clamp recordings were obtained from cells with overshooting action potential and a stable resting membrane potential. Each recorded neuron received a series of 500ms long current steps ranging from –100 to +500 pA in 20

pA increments. The current threshold for action potential was determined as the minimal current required for evoking an action potential during the current injection step. Spikes frequency was measured as the number of spikes evoked in response to 300pA current injection step.

Calcium imaging

Primary motor neurons were imaged at days 12-13 in vitro (12 DIV). Primary hippocampal neurons were imaged at 15 DIV. Cells plated on coverslips were incubated in 2 μ M Fluo-2 calcium indicator (Teflabs) for 45 minutes, in a solution containing: 129 mM NaCl, 4mM KCl, 1 mM MgCl₂, 2mM CaCl₂, 4.2mM glucose and 10mM HEPES, with pH adjusted to 7.4 with NaOH, and osmolarity to 320 mOsm adjusted with sucrose. Cells were washed twice and imaged at a wave length of 488nm with a Zeiss710 confocal laser scanning microscope, using a 40x objective. On each coverslip, 3 fields containing at least 10 neurons were chosen randomly for capture and analysis. At least 3 different coverslips were used per condition. Events in which $\Delta F/F > 0.5$ were included in the analysis.

Retrograde labeling of neuron subtypes

Motor neurons were back labeled via AAV-GFP injection into the mouse hindlimb Gastrocnemius (FF motor neurons) or Soleus (FR, S motor neurons) muscles. Mice were deeply anesthetized with ketamine/xylazine (0.25 mL, 10% (vol/vol), administered i.p.) before organ perfusion with PBS and 2.5% paraformaldehyde (PFA; as in (65)).

miRNA in situ hybridization (ISH)

miR-218 in situ hybridization in human tissues on 5 μ FFPE sections followed (66). miR-218 ISH mix, 30 pmol/100 μ L in hybridization buffer (Enzo Life Sciences), was placed on

tissue sections, heated to 60°C for 5 minutes and hybridized at 37°C overnight. Sections were washed (0.2X SSC with 2% bovine serum albumin) at 55°C for 10 minutes, treated with anti-digoxigenin – alkaline phosphatase conjugate (1:150 dilution in pH 7 Tris buffer; Roche) at 37°C for 30 minutes, develop with NBT/BCIP (ThermoFisher; 34042) until chromogen signal appeared at 15 – 30 minutes, counterstained with nuclear fast red for 3 to 5 minutes, rinsed and mounted with coverslips. Optical Density (OD) was calculated as log of (max intensity/Mean intensity).

miR-218 in situ hybridization in mouse tissues was performed on frozen spinal cord sections as in (67). Slides were treated with 2µg/ml Proteinase K, fixed in EDC (Sigma), acetylated in acetic anhydride/ triethanolamine solution and hybridized in a hybridization buffer containing 40nM of 5' + 3' DIG-labeled miR-218 or scrambleLNA probe (Exiqon). Slides were washed, incubated with alkaline phosphatase-conjugated goat-anti-DIG Fab fragments (1:1000, Roche) at 4°C overnight, developed with BCIP/NBT (Sigma), as in (68), mounted with Immu-mount (Shandon) and covered with a glass coverslip.

miR-218 lentiviruses

500bp flanking the pri-miR-218-2 sequence were purchased in pMX vectors (GeneArt, Invitrogen, table S3), and a 625bp fragment of the human pri-miR-218-1 were digested with BamHI-EcoRI and subcloned to pUltra-Hot vector (a gift from Malcolm Moore, Addgene plasmid # 24130) downstream of the human Ubiquitin C promoter and mCherry-P2A. To generate miR-218 inhibitor encoding lentivirus, an approximately 250bp fragment of the commercial inhibitor, miR-Zip-218 plasmid (SBI), driven by a U6 promoter was subcloned into pGEM vector (Promega) with Fw 5'-CGTACGTAAAGATGGCTGTGAGGGACAG-3' and Rev 5'-

CGTACGTAAGAGAGACCCAGTAGAAGCAAAAAG-3' primers, and then into the 3'LTR of pUltra-Hot vector using a SnaBI restriction site. Lentiviral particles were produced in HEK-293T cells, transfected with pUltra-Hot vector and with psPAX2 and pMD2.G packaging plasmids (a gift from Didier Trono, Addgene plasmid numbers 12259 and 12260). Supernatants were concentrated by ultracentrifugation, re-suspended in DMEM media (Gibco) and titrated. Primary neuronal cultures were infected at a multiplicity of infection (MOI) of 1 or of 10, on 1 DIV.

Luciferase assays

The rat KCND2 and KCNH1 3'UTRs were subcloned into psiCHECK2 vector (Promega) and transfected into HEK-293T cells with JET-PEI reagent (Poly Plus) together with miRVec-control and miRVec-218 plasmids, that were a gift from Reuven Agami (NKI, The Netherlands). For each well of a 24-well plate, a 50 ng psiCHECK2 plasmid DNA and 150 ng miRVec plasmid DNA were used; each well represents one technical replicate. 72 h post-transfection cells were harvested using the Dual luciferase reporter assay system (Promega).

Protein analysis

Primary motor neurons were harvested on E13.5, plated, transduced with lentiviruses and harvested after 5 days in culture. Cell pellet lysed in (50mM Tris pH7.4, 40mM NaCl, 1mM EDTA pH8, 0.5% TritonX-100, 50mM NaF, 10mM Na pyrophosphate, 10mM Na beta-glycerol phosphate, 1x phosphatase inhibitor (Roche) and 1x proteinase inhibitor (Roche)) and equal amounts of protein were loaded per lane for SDS-PAGE. After electro-transfer, blots were developed with rabbit anti Kv4.2 antibody (Proteintech Group, Rosemont, IL catalog# 21298-1-AP, RRID:AB_10733102, 1:2000), rabbit anti Kv10.1

antibody (Abcam, catalog# ab101174, RRID:AB_10862156, 1:500) and rabbit anti Tubulin Beta-III (TUBB3) (Biolegend, catalog# 802001, RRID:AB_2564645, 1:100,000) using chemiluminescence. Samples were loaded and quantified in duplicates on each gel. Densitometric analysis of specific bands was performed using ImageJ (NIH).

RNA analysis

Total RNA from cultured cells was isolated using DirectZol RNA miniprep Kit or miRNeasy micro Kit (Qiagen) and reverse transcribed using the miScript II RT Kit (Qiagen). Quantitative real-time PCR was performed with the LightCycler480 (Roche) or StepOnePlus (Thermo Fisher Scientific), in >3 independent biological repeats and technical duplicates. For miRNAs we used miScript SYBR Green PCR (Qiagen) or TaqMan microRNA assays (Thermo-Fisher Scientific). mRNA quantified with KAPA SYBR fast qPCR (KAPA biosystems). Hypoxanthine phosphoribosyltransferase 1 (Hprt) and β -actin were used as references for normalization of mRNA expression, and U6 for normalization of miRNA. Primer sequences are described in table S4. For small RNA next generation sequencing (NGS), cDNAs were prepared from 10 ng of total RNA using the QIAseq™ miRNA Library Kit and QIAseq miRNA NGS 48 Index IL (Qiagen). cDNA libraries were pooled and sequenced on a single NextSeq 500 flow cell (Illumina), with 75bp single read. Data was analyzed using the GeneGlobe analysis web tool (Qiagen), and further processed by in-house script for discovery of pre-miRNA sequences (source code: <https://github.com/TsviyaOlender/mir-218>). miR-218-5p reads were normalized to the reads of miR-214-3p miRNA mimic. For mRNA NGS, cDNAs were prepared following (69) and sequenced on one a single lane in a Hiseq2500 (Illumina) with 50bp single read. Fasta files for each sample were generated by the usage of Illumina CASAVA-1.8.2

software. Reads for each sample were mapped independently using TopHat2 version (v2.0.10) (70) against the mouse genome build mm9. Approximately, 85-90% mapping rate was observed. Only uniquely mapped reads were used to determine the number of reads falling into each gene with the HTSeq-count script (0.6.1p1) (71). Differentially expressed genes were calculated with the DESeq2 package (v1.4.5) (72). Genes that were expressed at least on one sample were considered. Differentially expressed genes, were determined by $P\text{-adj} < 0.05$ and an absolute fold change > 1.5 . Hierarchical clustering using Pearson dissimilarity and complete linkage was performed in order to explore a pattern of gene expression. Clustering analysis was performed with Matlab software (8.0.0.783).

NanoString

Human spinal cord RNA was extracted using Trizol, tested by NanoDrop (Thermo Scientific) for O.D. of 260/280 between 1.9 - 2.1 and hybridized for 18 hrs. against the nCounter Human v2 miRNA Panel (798 unique human miRNA barcodes) by the nCounter System (NanoString Technologies). Data from 280 fields of view per sample was analyzed with nSolver.

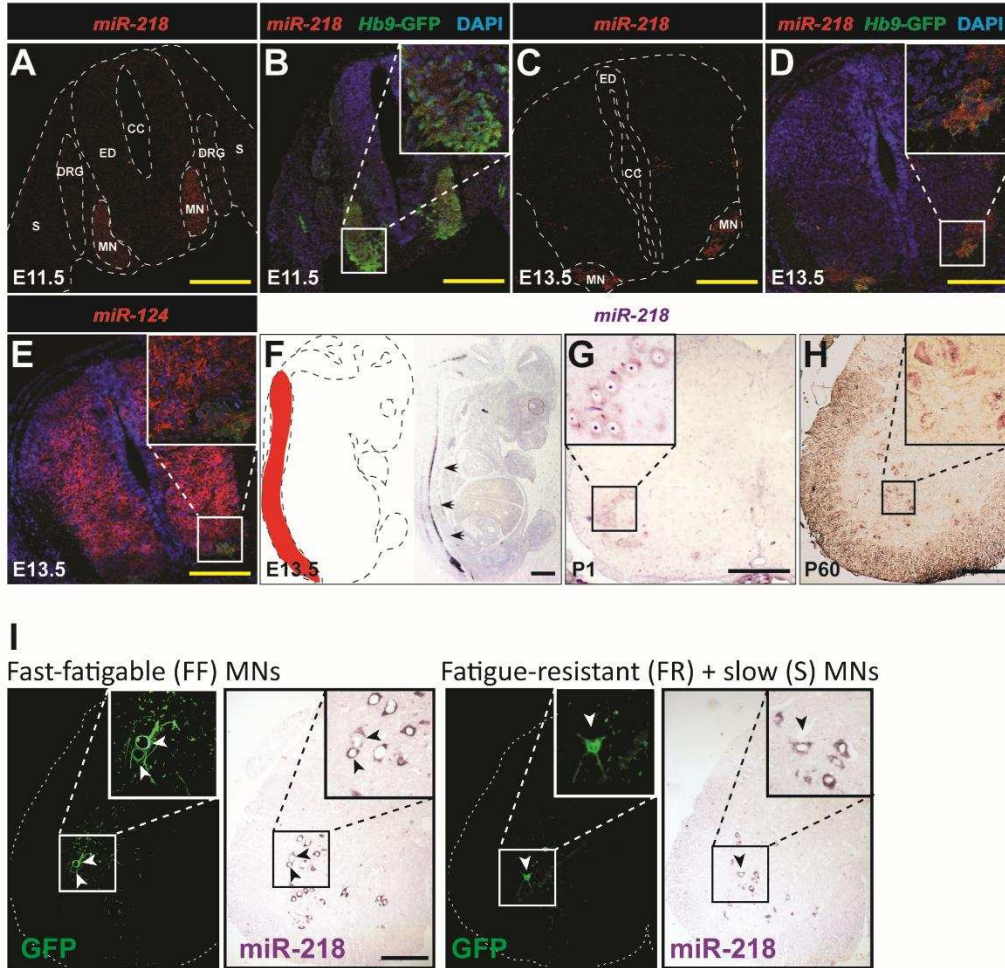


Fig. S1. miR-218 is highly and specifically expressed in human and murine spinal motor neurons. (A,C) miR-218 fluorescent in situ hybridization on transverse sections of mid-gestation mouse embryos (red) and (B,D) co-localization of motor neuron reporter transgene Hb9-FGP (green). CC-central canal; ED-ependymal layer; DRG-dorsal root ganglion; MN-motor neurons; S-somites. (E) In situ hybridization of pan-neuronal miR-124. Merged micrographs depict nuclei by DAPI counterstaining. (F) Alkaline Phosphatase chromogen development of miR-218 in situ hybridization on a mid-sagittal section of E13.5 mouse embryo. Arrowheads indicate the localization of motor neurons. miR-218 in situ hybridization on transverse hemisections of (G) newborn or (H) adult mouse spinal cord. Inset - large motor perikaryon cluster. (I) Transverse hemisections of adult mouse spinal cord, retrogradely labeled by AAV9-GFP injection into the lateral gastrocnemius (FF motor neurons, left) or soleus (FR/S motor neurons, right) and accompanied by miR-218 in situ hybridization. Arrowheads depict soma of GFP-labeled, lumbar motor neurons. Scale bars - 200 μm.

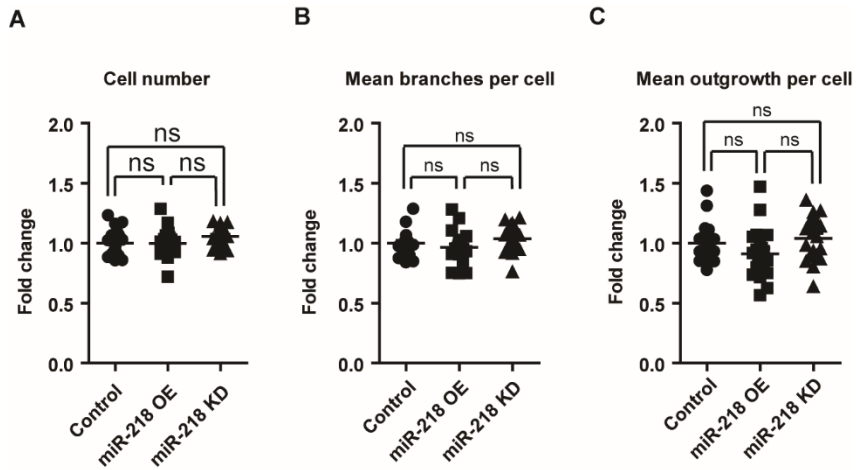


Fig. S2. High content analysis (HCA) of neuronal morphology following miR-218 perturbation. Primary motor neurons were plated in a 384-well plate, transduced with control, miR-218 OE or miR-218 inhibitor encoding lentiviruses and stained at 4 DIV. Neuron-specific class III beta-tubulin (Tuj1) was used to visualize neuronal processes and DAPI for visualization of nuclei. Phenotypic parameters were quantified using MetaXpress High-Content Image Acquisition and Analysis Software (Molecular Devices) set to identify and measure only cellular processes connected to cell bodies. **(A)** Cell number. Only nuclei of cells expressing Tuj1 were counted. **(B)** Mean number of branches per cell. **(C)** Mean axonal outgrowth per cell. Data normalized to control virus transduced cells. $n=24$ independent wells per experimental condition, in two technical duplicates, each. This experiment was repeated 3 independent times with similar results. Error bars, mean \pm SEM. One-way ANOVA followed by Bonferroni's multiple comparison test. ns – non-significant.

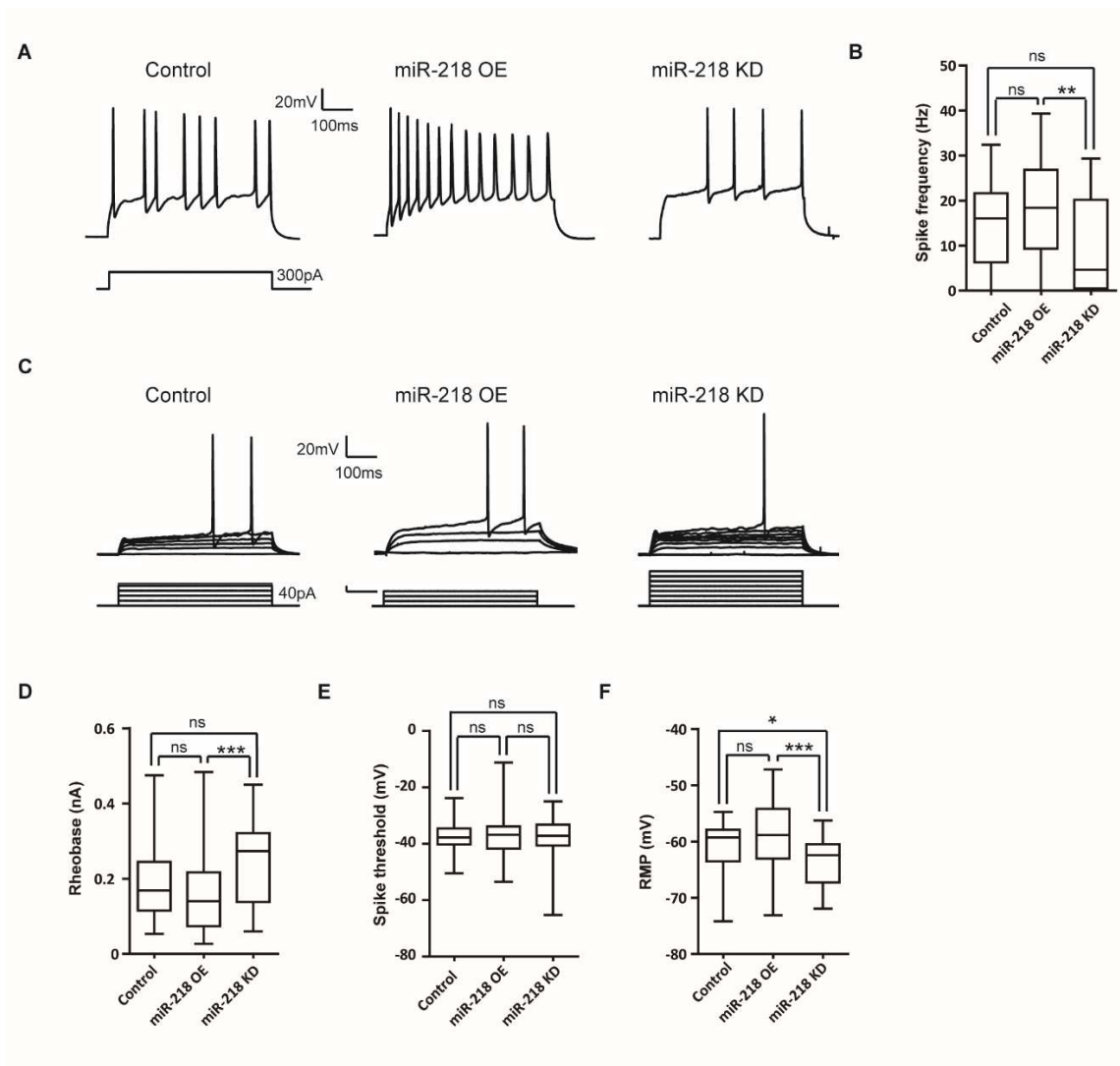


Fig. S3. miR-218 regulates intrinsic excitability. (A) Representative traces depicting repetitive firing, following miR-218 perturbation. Recordings of rat hippocampal neurons, transduced with lentiviruses encoding mCherry alone (control), miR-218 overexpression (miR-218 OE) or a miR-218 knockdown (miR-218 KD) inhibitor, following injection of 300pA depolarizing current for 500ms. Injected current amplitude and duration are illustrated in the lower pane. (B) Quantification of firing rates. (C) Representative traces depicting rheobase - current input required to generate action potential. (D) Quantification of rheobase; (E) spike threshold; (F) resting membrane potential (RMP). Control, n=44; miR-218 OE, n=65; miR-218 KD, n=30. Data was combined from 4 independent experiments. Kruskal-Wallis test and Dunn's multiple comparison test. Error bars, mean \pm SEM, * P<0.05; ** P<0.01; *** P<0.001; ns - non-significant.

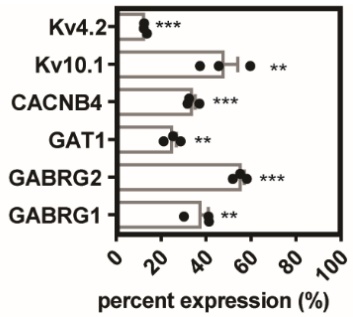


Fig. S4. qPCR validation of miR-218 target knockdown. Targeting and non-targeting control siRNAs (Integrated DNA Technologies, Inc.) were encapsulated in Neuro9™ nanoparticles (Precision NanoSystems, Inc.). Primary motor neurons were transfected with siRNA at a final concentration of 1µg/ml, at 9 DIV. At 12 DIV RNA was extracted and expression of miR-218 targets was analyzed by qPCR. Data normalized to average expression of HPRT and β-actin. n=3 independent wells per experimental condition, in two technical duplicates, each. Error bars, mean ± SEM. Two-sided student t-test. ** P<0.01; *** P<0.001.

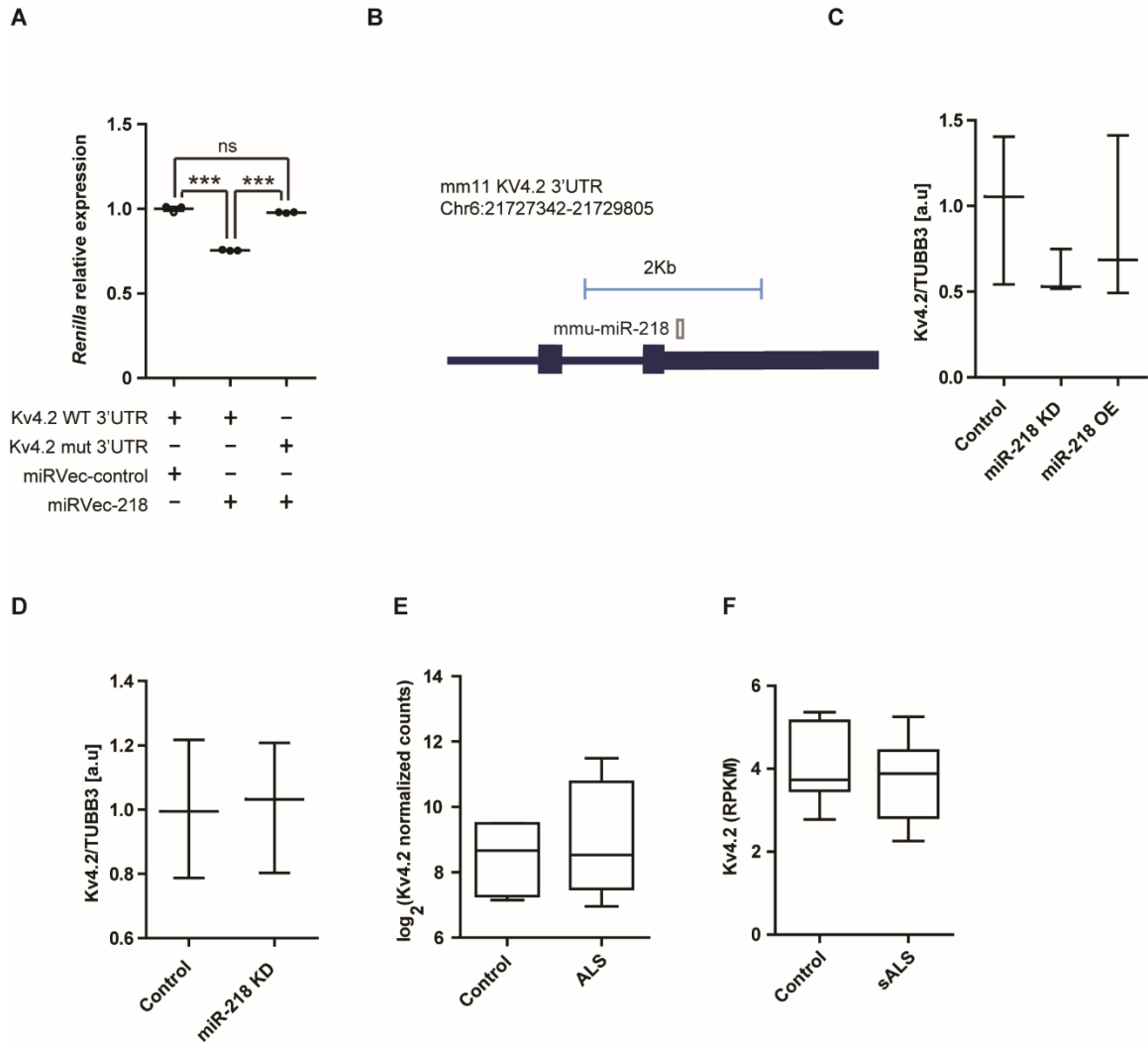


Fig. S5. Evaluation of miR-218 upstream of the mRNA encoding for the potassium channel Kv4.2 (Kcnd2). (A) Relative Renilla luminescence upstream of a wild-type Kv4.2 3'UTR or a mutated 3'UTR that is insensitive to miR-218, normalized to co-expressed firefly luciferase and to a negative control miRNA vector. n=3 independent wells per experimental condition. One-way ANOVA followed by Bonferroni's multiple comparison test. Error bars, mean \pm SEM. *** P<0.001. (B) AGO2 CLEAR-CLIP experiment did not identify a miR-218:Kv4.2 3'UTR chimera in mouse cortex (29), as opposed to the miR-218:Kv10.1 3'UTR chimera in main Fig. 3J. (C,D) Western blot studies of Kv4.2 protein expression, in primary rat motor neurons, presented as boxplot (median, upper / lower quartiles & extreme points), upon (C) miR-218 knockdown (miR-218 KD, n=3) or overexpression (miR-218 OE, n=3), relative to Control (n=3). One-way ANOVA followed by Newman-Keuls multiple comparison test, and a validation study of (D) miR-218 KD

(n=3), relative to Control (n=3). Two-sided student t-test. **(E)** Kv4.2 mRNA expression, as log₂ normalized counts, from NGS study of induced ALS motor neurons (n=4 different donors in duplicates) or non-neurodegeneration controls (n=3 different donors in duplicates; (30)). Box-Plots depict median, upper / lower quartiles & extreme points, DESeq analysis. Non-significant difference. **(F)** Kv4.2 mRNA expression, as Reads Per Kilobase Million (RPKM) from NGS study of laser capture microdissection-enriched surviving motor neurons from lumbar spinal cords of patients with sALS with rostral onset and caudal progression (n=12) and non-neurodegeneration controls (n=9; (21), GSE76220). Box-Plots depict median, upper / lower quartiles & extreme points, two-sided student's t-test. Non-significant difference.

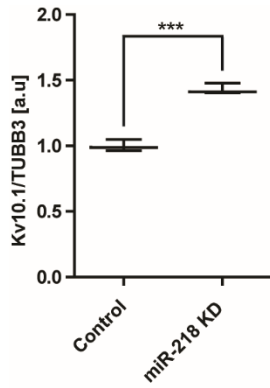


Fig. S6. Kv10.1 (Kcnh1) protein quantification by western blot, following miR-218 KD. A western blot validation study of Kv10.1 protein expression upon miR-218 KD (n=3), in primary rat motor neurons, relative to Control (n=3). Box-Plots depict median, upper / lower quartiles & extreme points, two-sided student t-test. *** P<0.001.

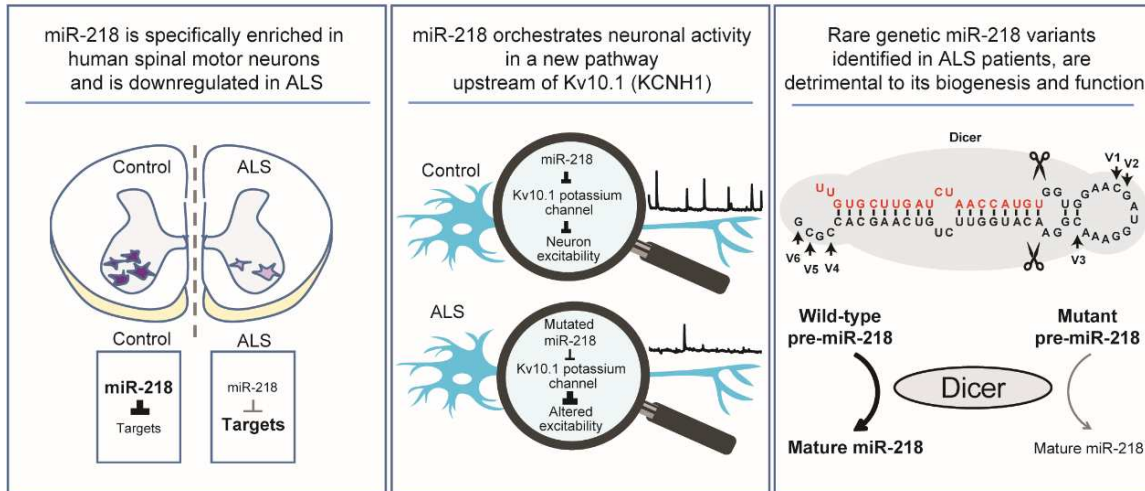


Fig. S7. A summary diagram of key observations. (left) Human pathology: miR-218 expression is reduced in ALS ventral horns, because of both molecular downregulation and of motor neuron loss. Accordingly, mRNA targets of miR-218 are reciprocally upregulated (de-repressed). miR-218 might serve as a biomarker of motor neuron mass. (center) miR-218 regulates neuronal activity upstream of the voltage gated potassium channel Kv10.1 (Kcnh1). (right) Human genetics: rare genetic variants identified in patients with ALS, in the sequence of the pre-miR-218-2 gene, dysregulate miR-218 biogenesis and impair regulation of neuron activity. miR-218 contributes to motor neuron specificity and its function may be particularly susceptible to failure in motor neuron diseases. Therefore, the work connects human genetics and human neuropathology to motor neuron-specific functions via a small non coding RNA.

Table S1. Identified hsa-miR-218-2 variants.

Variant	Position (GRCh37/hg19)	Ref	Alt	dbSNP ID	Minor Allele Frequency						
					Discovery		Replication		TOPMed	Total	
					cases (n= 4281)	controls (n=1838)	cases (n=3457)	controls (n=7034)	controls (n=62784)	cases (n=7738)	controls (n=71656)
V1	Chr5:168,195,208 (-)	C	A	rs751147155	2.3×10^{-4}	0				1.3×10^{-4}	0
V2	Chr5:168,195,207 (-)	G	A	rs374716278	2.3×10^{-4}	0	2.9×10^{-4}	0	0.5×10^{-4}	2.6×10^{-4}	0.4×10^{-4}
V3	Chr5:168,195,199 (-)	C	T	rs773402384	0	5.4×10^{-4}				0	0.1×10^{-4}
V4	Chr5:168,195,176 (-)	C	T	rs368624931	2.3×10^{-4}	0	2.9×10^{-4}	0		2.6×10^{-4}	0
V5	Chr5:168,195,174 (-)	C	T	rs140638702	9.3×10^{-4}	5.4×10^{-4}	11.6×10^{-4}	4.3×10^{-4}	3.2×10^{-4}	10.3×10^{-4}	3.3×10^{-4}
V6	Chr5:168,195,173 (-)	G	A	rs780192152	4.7×10^{-4}	0	0	1.4×10^{-4}	1.1×10^{-4}	2.6×10^{-4}	1.1×10^{-4}
V7	Chr5:168,195,198 (-)	G	A	rs770316009					0.5×10^{-4}	0	0.4×10^{-4}
V8	Chr5:168,195,196 (-)	A	G	rs372358902					0.5×10^{-4}	0	0.4×10^{-4}
V9	Chr5:168,195,175 (-)	G	A	rs758061075					0.2×10^{-4}	0	0.1×10^{-4}
Total					21.0×10^{-4}	10.9×10^{-4}	17.4×10^{-4}	5.7×10^{-4}	5.9×10^{-4}	19.4×10^{-4}	6.0×10^{-4}

Ref, Reference allele; Alt, Alternate allele.

Table S2. DsiRNA sequences employed in the study.

Oligo name	S-strand	AS-strand
has-miR-214-3p mimic	5'-phos-rArCrArGrCrArGrGrCrArCrArGrArCrArGrGrCmAmGmU-3'	5'-mUmGrCmCrUmGrUmCrUmGrUmGrCmCrUmGrCmUrGrU-3'
NC5 siRNA	5'-rCrGrCrGrArCrUrArUrArCrGrCrGrCrArArUrArUmGmGrU-3'	5'-rUmCrCmArUmArAmArGmUrAmGrGmArAmArCmArCmUrAmCA-3'
Rat Cacnb4 siRNA	5'-mGmUrCmUrAmCrCrUrGrArGmCrAmUrGmUrUmGrArArArUrCmAA-3'	5'-rUrUmGrArUrUrUrCmArAmCrAmUrGrCrUrCrArGrGrUrAmGrAmCmUmU-3'
Rat Kend2 siRNA	5'-mUmGrCmArAmGrArArCrUrCmArGmUrAmCrAmArUrUrCrArGmAT-3'	5'-rArUmCrUrGrArArUmUrGmUrAmCrUrGrArGrUrUrCrUrUmGrCmAmCmG-3'
Rat Kenh1 siRNA	5'-mGmCrUmGrAmGrArGrGrArUmCrAmUrUmUrCmArArArArCrAmAA-3'	5'-rUrUmUrGrUrUrUrUmGrAmArAmUrGrArUrCrCrUrCrUrCmArGmCmUmU-3'
Rat Slc6a1 siRNA	5'-rCrCrArArArUrGrArCrArGrArUrGrGrCrUrArGrArCrAAG-3' 5'-rCrCrCrArUrGrUrArGrCrArArArGrCrGrUrArUrArUrGrUCT-3' 5'-rArCrCrUrUrArUrArGrArGrCrArCrArArCrGrUrUrArArGGG-3' 5'-rGrGrArGrArArGrArCrUrCrArUrArGrCrArGrArGrArArCTA-3' 5'-rCrArArArUrGrArUrArUrCrArCrArArCrUrArGrArGrCrACG-3' 5'-rCrCrUrUrArArUrArArCrUrArUrGrUrGrArArUrArArCTG-3' 5'-rGrCrArArArCrArGrCrCrUrArUrCrCrArGrArArGrArGrCTC-3' 5'-rArGrCrArUrCrArArGrCrArCrArCrUrGrUrArGrArGrArATG-3' 5'-rCrCrArGrArGrGrGrArArGrArArGrArUrArArUrUrGrUrATT-3'	5'-rCrUrUrGrUrCrUrArGrCrCrCrArUrCrUrGrUrCrArUrUrUrGrGrUrG-3' 5'-rArGrArCrArUrArUrArCrGrCrUrUrUrGrCrUrArCrArUrGrGrGrArG-3' 5'-rCrCrCrUrUrArArCrGrUrUrGrUrGrCrUrCrUrArUrArArGrGrUrUrA-3' 5'-rUrArGrUrUrCrUrCrUrGrCrUrArUrGrArGrUrCrUrUrCrUrCrUrA-3' 5'-rCrGrUrGrCrUrCrUrArGrUrUrGrUrGrArUrArUrCrArUrUrUrGrArU-3' 5'-rCrArGrUrUrArUrUrCrArCrCrArUrArGrUrUrArUrUrArArGrGrArU-3' 5'-rGrArGrCrUrCrUrUrCrUrGrGrArUrArGrGrCrUrGrUrUrUrGrCrUrG-3' 5'-rCrArUrUrCrUrCrUrArCrArGrUrGrUrGrCrUrUrGrArUrGrCrUrCrU-3' 5'-rArArUrArCrArArUrUrArUrCrUrUrCrUrUrCrCrCrUrCrUrGrGrCrC-3'

	<p>5'- rGrCrArCrArCrCrArGrUrUrCrUrUr GrCrArArUrArArGrCTA-3'</p> <p>5'- rGrCrArGrUrArUrArUrUrCrArUr GrUrUrUrGrArArArGCA-3'</p> <p>5'- rGrArArCrArUrUrUrArUrUrArCrAr UrUrGrUrCrArUrCrATC-3'</p> <p>5'- rGrArUrUrUrArUrUrCrUrCrArGrAr ArCrArCrCrArArGrUAA-3'</p> <p>5'- rArGrArArGrArUrArArUrUrGrUrAr UrUrArUrCrArUrArUAT-3'</p> <p>5'- rCrArGrUrUrCrUrUrGrCrArArUrAr ArGrCrUrArUrCrUrCCC-3'</p> <p>5'- rCrArCrCrArArGrUrArArArUrUrUr ArUrCrUrCrUrArUrATA-3'</p> <p>5'- rGrArUrUrGrCrUrCrUrGrGrGrArAr GrCrUrArCrArArCrUCT-3'</p> <p>5'- rCrArArGrUrCrUrUrUrUrUrGrAr GrArUrArArArUrGrCAG-3'</p> <p>5'- rCrArArArUrGrArUrArUrCrArCrAr ArCrUrArGrArGrCrACG-3'</p> <p>5'- rUrCrGrArUrGrUrUrCrUrUrUrGrAr UrGrGrArArArArCrUGA-3'</p>	<p>5'- rUrArGrCrUrUrArUrUrGrCrArArGrAr ArCrUrGrGrUrGrUrGrCrUrG-3'</p> <p>5'- rUrGrCrUrUrUrCrArArArCrArUrGrAr ArArUrArUrArCrUrGrCrArU-3'</p> <p>5'- rGrArUrGrArUrGrArCrArArUrGrUrAr ArUrArArArUrGrUrUrCrArG-3'</p> <p>5'- rUrUrArCrUrUrGrGrUrGrUrUrCrUrGr ArGrArArUrArArArUrCrCrU-3'</p> <p>5'- rArUrArUrArUrGrArUrArArUrArCrAr ArUrUrArUrCrUrUrCrUrUrC-3'</p> <p>5'- rGrGrGrArGrArUrArGrCrUrUrArUrUr GrCrArArGrArArCrUrGrGrU-3'</p> <p>5'- rUrArUrArUrArGrArGrArUrArArArUr UrUrArCrUrUrGrGrUrGrUrU-3'</p> <p>5'- rArGrArGrUrUrGrUrArGrCrUrUrCrCr CrArGrArGrCrArArUrCrArG-3'</p> <p>5'- rCrUrGrCrArUrUrUrArUrCrUrCrArAr ArArArArGrArCrUrUrGrUrU-3'</p> <p>5'- rCrGrUrGrCrUrCrUrArGrUrUrGrUrGr ArUrArUrCrArUrUrUrGrArU-3'</p> <p>5'- rUrCrArGrUrUrUrUrCrCrArUrCrArAr ArGrArArCrArUrCrGrArG-3'</p>
Rat Gabrb2 siRNA	<p>5'- rArCrCrUrArCrUrUrCrCrUrGrArAr UrGrArUrArArGrArAGT-3'</p> <p>5'- rGrArArUrArUrGrCrUrUrUrGrGrUr CrArArCrUrArCrArUCT-3'</p> <p>5'- rGrCrArCrUrCrUrUrGrArGrArUrAr ArArArArArUrGrArGAT-3'</p> <p>5'- rCrUrGrArArGrUrCrArArUrArUrGr GrArCrUrArCrArCrCTT-3'</p> <p>5'- rGrUrGrGrCrArGrUrArGrGrArArUr GrArArCrArUrUrGrATA-3'</p>	<p>5'- rArCrUrUrCrUrUrArUrCrArUrUrCrAr GrGrArArGrUrArGrGrUrGrU-3'</p> <p>5'- rArGrArUrGrUrArGrUrUrGrArCrCrAr ArArGrCrArUrArUrUrCrCrA-3'</p> <p>5'- rArUrCrUrCrArUrUrUrUrUrArUrCr UrCrArArGrArGrUrGrCrUrG-3'</p> <p>5'- rArArGrGrUrGrUrArGrUrCrCrArUrAr UrUrGrArCrUrUrCrArGrArA-3'</p> <p>5'- rUrArUrCrArArUrGrUrUrCrArUrUrCr CrUrArCrUrGrCrCrArCrArG-3'</p>

	<p>5'- rCrArArCrUrGrArUrGrArCrArUrUr GrArGrUrUrUrUrArCTG-3'</p> <p>5'- rCrArUrCrArGrArArGrCrArGrUrAr ArUrGrGrGrArCrUrUGG-3'</p> <p>5'- rUrArCrUrCrArGrCrArCrUrCrUrUr GrArGrArUrArArAAA-3'</p> <p>5'- rGrUrCrCrUrGrArCrGrArUrGrArCr CrArCrArArUrCrArATA-3'</p> <p>5'- rGrArUrArArGrArArGrUrCrArUrUr UrGrUrArCrArUrGrGAG-3'</p> <p>5'- rArGrArCrUrGrUrCrCrUrArCrArAr UrGrUrArArUrCrCrCTT-3'</p> <p>5'- rArCrUrUrCrArUrCrCrUrGrCrArGr ArCrArUrArCrArUrGCC-3'</p> <p>5'- rUrCrArArUrGrArCrCrCrUrArGrUr ArArUrArUrGrUrCrGCT-3'</p> <p>5'- rGrGrArArUrArUrGrCrUrUrUrGrGr UrCrArArCrUrArCrATC-3'</p> <p>5'- rGrGrArArUrGrArArCrArUrUrGrAr UrArUrCrGrCrCrArGCA-3'</p> <p>5'- rCrCrArCrArUrCrArGrArArGrCrAr GrUrArArUrGrGrGrACT-3'</p> <p>5'- rArGrArArArGrCrUrGrCrUrArArUr GrCrCrArArCrArArCGA-3'</p> <p>5'- rGrGrArCrUrArCrArCrCrUrUrGrAr CrCrArUrGrUrArUrUTC-3'</p> <p>5'- rArGrArArUrCrArCrArArCrUrArCr ArGrCrUrGrCrCrUrGCA-3'</p> <p>5'- rArGrArUrUrGrUrCrCrCrUrArArGr CrUrUrUrArArGrCrUGA-3'</p>	<p>5'- rCrArGrUrArArArArCrUrCrArArUrGr UrCrArUrCrArGrUrUrGrUrA-3'</p> <p>5'- rCrCrArArGrUrCrCrCrArUrUrArCrUr GrCrUrUrCrUrGrArUrGrUrG-3'</p> <p>5'- rUrUrUrUrUrUrArUrCrUrCrArArGrAr GrUrGrCrUrGrArGrUrArArG-3'</p> <p>5'- rUrArUrUrGrArUrUrGrUrGrGrUrCrAr UrCrGrUrCrArGrGrArCrArG-3'</p> <p>5'- rCrUrCrCrArUrGrUrArCrArArArUrGr ArCrUrUrCrUrUrArUrCrArU-3'</p> <p>5'- rArArGrGrGrArUrUrArCrArUrUrGrUr ArGrGrArCrArGrUrCrUrCrU-3'</p> <p>5'- rGrGrCrArUrGrUrArUrGrUrCrUrGrCr ArGrGrArUrGrArArGrUrArG-3'</p> <p>5'- rArGrCrGrArCrArUrArUrUrArCrUrAr GrGrGrUrCrArUrUrGrArCrA-3'</p> <p>5'- rGrArUrGrUrArGrUrUrGrArCrCrArAr ArGrCrArUrArUrUrCrCrArG-3'</p> <p>5'- rUrGrCrUrGrGrCrGrArUrArUrCrArAr UrGrUrUrCrArUrUrCrCrUrA-3'</p> <p>5'- rArGrUrCrCrCrArUrUrArCrUrGrCrUr UrCrUrGrArUrGrUrGrGrCrC-3'</p> <p>5'- rUrCrGrUrUrGrUrUrGrGrCrArUrUrAr GrCrArGrCrUrUrUrCrUrCrA-3'</p> <p>5'- rGrArArArUrArCrArUrGrGrUrCrArAr GrGrUrGrUrArGrUrCrCrArU-3'</p> <p>5'- rUrGrCrArGrGrCrArGrCrUrGrUrArGr UrUrGrUrGrArUrUrCrUrGrA-3'</p> <p>5'- rUrCrArGrCrUrUrArArArGrCrUrUrAr GrGrGrArCrArArUrCrUrGrG-3'</p>
Rat Gabrg1 siRNA	<p>5'- rGrUrCrUrArCrCrArGrUrUrArArAr ArUrCrUrGrArArUrCAT-3'</p>	<p>5'- rArUrGrArUrUrCrArGrArUrUrUrUrAr ArCrUrGrGrUrArGrArCrUrU-3'</p>

5'-
rArArArUrCrUrGrArArUrCrArUrUr
UrGrGrUrCrArUrArUGA-3'

5'-
rCrUrGrGrCrUrUrArGrUrCrCrArAr
UrArUrArArUrCrArCTT-3'

5'-
rCrUrArCrCrArGrUrUrArArArArUr
CrUrGrArArUrCrArUTT-3'

5'-
rArCrUrGrGrArArUrUrUrUrCrArAr
GrCrUrArUrGrGrArUAC-3'

5'-
rCrArGrUrArArUrUrGrArArArCrUr
GrArUrGrUrUrUrArUGT-3'

5'-
rGrUrGrArGrGrUrUrGrArUrArUrUr
CrUrUrGrUrUrArCrUAA-3'

5'-
rCrCrUrArArGrGrUrUrUrCrUrUrAr
CrGrUrGrArCrArGrCAA-3'

5'-
rCrUrUrGrCrArUrUrArUrUrUrUrAr
CrUrArGrUrArArCrAAT-3'

5'-
rGrArArUrUrArUrUrCrArGrGrUrUr
ArArUrUrUrArCrCrUAA-3'

5'-
rGrGrCrUrArUrGrArUrArArCrArAr
ArCrUrUrCrGrUrCrCAG-3'

5'-
rUrGrArCrArArCrCrCrUrCrArGrUr
ArCrArArUrCrGrCrUAG-3'

5'-
rCrCrUrUrUrGrUrArGrGrGrUrUrAr
ArGrArArArUrUrCrAAC-3'

5'-
rGrGrArGrUrCrArArArCrUrArGrAr
GrGrArGrUrGrArGrGTT-3'

5'-
rGrGrArArCrUrCrArArGrGrArArAr
UrCrUrGrArUrGrCrGCA-3'

5'-
rCrCrCrArCrArGrUrArArUrUrGrAr
ArArCrUrGrArUrGrUTT-3'

5'-
rCrCrArUrGrArArCrArArCrArUrUr
UrCrUrArUrGrCrCrUCA-3'

5'-
rUrCrArUrArUrGrArCrCrArArArUrGr
ArUrUrCrArGrArUrUrUrUrA-3'

5'-
rArArGrUrGrArUrUrArUrArUrUrGrGr
ArCrUrArArGrCrCrArGrArU-3'

5'-
rArArArUrGrArUrUrCrArGrArUrUrUr
UrArArCrUrGrGrUrArGrArC-3'

5'-
rGrUrArUrCrCrArUrArGrCrUrUrGrAr
ArArArUrUrCrCrArGrUrGrG-3'

5'-
rArCrArUrArArArCrArUrCrArGrUrUr
UrCrArArUrUrArCrUrGrUrG-3'

5'-
rUrUrArGrUrArArCrArArGrArArUrAr
UrCrArArCrCrUrCrArCrUrC-3'

5'-
rUrUrGrCrUrGrUrCrArCrGrUrArArGr
ArArArCrCrUrUrArGrGrUrA-3'

5'-
rArUrUrGrUrUrArCrUrArGrUrArArAr
ArUrArArUrGrCrArArGrUrU-3'

5'-
rUrUrArGrGrUrArArArUrUrArArCrCr
UrGrArArUrArArUrUrCrUrU-3'

5'-
rCrUrGrGrArCrGrArArGrUrUrUrGrUr
UrArUrCrArUrArGrCrCrUrU-3'

5'-
rCrUrArGrCrGrArUrUrGrUrArCrUrGr
ArGrGrGrUrUrGrUrCrArUrA-3'

5'-
rGrUrUrGrArArUrUrUrCrUrUrArArCr
CrCrUrArCrArArArGrGrCrA-3'

5'-
rArArCrCrUrCrArCrUrCrCrUrCrUrAr
GrUrUrUrGrArCrUrCrCrArC-3'

5'-
rUrGrCrGrCrArUrCrArGrArUrUrUrCr
CrUrUrGrArGrUrUrCrCrUrG-3'

5'-
rArArArCrArUrCrArGrUrUrUrCrArAr
UrUrArCrUrGrUrGrGrUrC-3'

5'-
rUrGrArGrGrCrArUrArGrArArArUrGr
UrUrGrUrUrCrArUrGrGrArA-3'

5'- rCrCrArArUrArUrArArUrCrArCrUr UrCrGrArUrUrUrCrATA-3'	5'- rUrArUrGrArArArUrCrGrArArGrUrGr ArUrUrArUrArUrUrGrGrArC-3'
5'- rGrGrArUrGrGrGrCrUrArUrUrUrCr ArCrArArUrUrCrArGAC-3'	5'- rGrUrCrUrGrArArUrUrGrUrGrArArAr UrArGrCrCrCrArUrCrCrGrU-3'
5'- rArArCrArUrGrGrArGrUrArCrArCr GrArUrArGrArCrArUCA-3'	5'- rUrGrArUrGrUrCrUrArUrCrGrUrGrUr ArCrUrCrCrArUrGrUrUrUrA-3'

rA rC rG rU = RNA; mA mC mG mU = 2'OMe RNA ; A G C T = DNA; phos = phosphate.

Table S3. Synthetic miR-218 sequences used for cloning into pMA-T vectors.

Variant	Synthetic gene sequence
WT miR-218	5'- CTGTGTCTCCCGCGGATCCGCGCTGGGGTGGGGCACAAGGGCAGCAGGGC TGCAATCTTCGGAAGTGTTCCAGTGGAAACCCCACTCCTGATACTAATCACG CTCAGTGGGGGCCTGCTCCGGCTTCCGCTTCTCCACGCTGCTTCCTCTGAG CGTCCTGTCTCTCTCTGACGCTGCTTCCTGACCTTGACTCTGACCAGTC GCTGCGGGGCTTTCCTTTGTGCTTGATCTAACCATGTGGTGGAAACGATGGA AACGGAACATGGTTCTGTCAAGCACCGCGGAAAGCACCGTGCTCTCCTGC AGCATGGCCCGCCACCGCCGCCACCACCGCTGGACACCTCTCCTCTGCTCT GGAGCACCGCAGCCACCACCTGCCAGACCCACCTCTCCAGTCTCAACT CACCAAAGGCAGGAGGGTAGGAGTCTCAAAGGATGCAGATACAGAGGGA AATGGGTCTGGAGAAGCACCCCTGGCCGGAATTCCGGGGAAAGAGAT-3'
V2	5'- CTGTGTCTCCCGCGGATCCGCGCTGGGGTGGGGCACAAGGGCAGCAGGGC TGCAATCTTCGGAAGTGTTCCAGTGGAAACCCCACTCCTGATACTAATCACG CTCAGTGGGGGCCTGCTCCGGCTTCCGCTTCTCCACGCTGCTTCCTCTGAG CGTCCTGTCTCTCTCTGACGCTGCTTCCTGACCTTGACTCTGACCAGTC GCTGCGGGGCTTTCCTTTGTGCTTGATCTAACCATGTGGTGGAAACATGGA AACGGAACATGGTTCTGTCAAGCACCGCGGAAAGCACCGTGCTCTCCTGC AGCATGGCCCGCCACCGCCGCCACCACCGCTGGACACCTCTCCTCTGCTCT GGAGCACCGCAGCCACCACCTGCCAGACCCACCTCTCCAGTCTCAACT CACCAAAGGCAGGAGGGTAGGAGTCTCAAAGGATGCAGATACAGAGGGA AATGGGTCTGGAGAAGCACCCCTGGCCGGAATTCCGGGGAAAGAGAT-3'
V5	5'- CTGTGTCTCCCGCGGATCCGCGCTGGGGTGGGGCACAAGGGCAGCAGGGC TGCAATCTTCGGAAGTGTTCCAGTGGAAACCCCACTCCTGATACTAATCACG CTCAGTGGGGGCCTGCTCCGGCTTCCGCTTCTCCACGCTGCTTCCTCTGAG CGTCCTGTCTCTCTCTGACGCTGCTTCCTGACCTTGACTCTGACCAGTC GCTGCGGGGCTTTCCTTTGTGCTTGATCTAACCATGTGGTGGAAACGATGGA AACGGAACATGGTTCTGTCAAGCACCGTGGAAAGCACCGTGCTCTCCTGC AGCATGGCCCGCCACCGCCGCCACCACCGCTGGACACCTCTCCTCTGCTCT GGAGCACCGCAGCCACCACCTGCCAGACCCACCTCTCCAGTCTCAACT CACCAAAGGCAGGAGGGTAGGAGTCTCAAAGGATGCAGATACAGAGGGA AATGGGTCTGGAGAAGCACCCCTGGCCGGAATTCCGGGGAAAGAGAT-3'
Vall	5'- CTGTGTCTCCCGCGGATCCGCGCTGGGGTGGGGCACAAGGGCAGCAGGGC TGCAATCTTCGGAAGTGTTCCAGTGGAAACCCCACTCCTGATACTAATCACG CTCAGTGGGGGCCTGCTCCGGCTTCCGCTTCTCCACGCTGCTTCCTCTGAG CGTCCTGTCTCTCTCTGACGCTGCTTCCTGACCTTGACTCTGACTAGTCG CTGCGGGGCTTTCCTTTGTGCTTGATCTAACCATGTGGTGGAAAATGGAA ACGGAACATGGTTCTGTCAAGCACTGTAGAAAGCACCGTGCTCTCCTGCA GCATGGCCCGCCACCGCCGCCACCACCGCTGGACACCTCTCCTCTGCTCTG GAGCACCGCAGCCACCACCTGCCAGACCCACCTCTCCAGTCTCAACTC ACCAAAGGCAGGAGGGTAGGAGTCTCAAAGGATGCAGATACAGAGGGAA ATGGGTCTGGAGAAGCACCCCTGGCCGGAATTCCGGGGAAAGAGAT-3'

Vdead	5'- CTGTGTCTCCCGCGGATCCGCGCTGGGGTGGGGCACAAGGGCAGCAGGGC TGCAATCTTCGGAAGTGTTCCAGTGGAACCCCACTCCTGATACTAATCACG CTCAGTGGGGGCCTGCTCCGGCTTCCGCTTCTCCACGCTGCTTCCTCTGAG CGCTCCTGTCTCTCTCTGACGCTGCTTCCTGACCTTGACTCTGACCAGTC GCTGCGGG AACCAATT TGTGCTTGATCTAACCATGTGGTGGAAACGATGG AAACGGAACATGGTTCTGTCAAGCACCGCG GAAAGCACCGTGCTCTCCTG CAGCATGGCCCGCCACCGCCGCCACCACCGCTGGACACCTCTCCTCTGCTC TGGAGCACCGCAGCCACCACCTGCCAGACCCACCTCTCCAGTCTCAAC TCACCAAAGGCAGGAGGGTAGGAGTCTCAAAGGATGCAGATACAGAGGG AAATGGGTCTGGAGAAGCACCTGGCCGGAATTCCGGGGAAAGAGAT-3'
-------	---

pre-miR-218 sequence (Blue); variants (Red)

Table S4. Primers used for quantitative real-time PCR.

Gene	Forward (5' to 3')	Reverse (5' to 3')
miR-218-5p	TTGTGCTTGATCTAACCATGT	NA
RNU6B (U6)	GATGACACGCAAATTCGTGAA	NA
hHPRT	ACTTTGCTTTCCTTGGTCAGGCAGT	CGTGGGGTCCTTTTCACCAGCA
hGAPDH	TTCTTTTTCGTCGCCAGCCGA	GTGACCAGGCGCCCAATACGA
hHB9	GGAGCACCAGTTCAAGCTCA	AATCTTCACCTGGGTCTCGGT
hISL1	CAGTCCAGAGAGACACGACG	AATTGACCAGTTGCTGAAAAGC
hChAT	AAGGAAGGTCCACACCTCTG	TCAGACACCAAGTGTCGCAT
Rat Hpvt	CGAGATGCTATGAAGGAGATGG	GTAATCCAGCAGGTCAGCAAAG
Rat Gapdh	CCTTTAGTGGGCCCTCGG	GCCTGGAGAAACCTGCCAAG
Rat Kcnd2	CAAGTTCACCAGCATCCCT	CCCGAAAATCTTCCCTGCTAT
Rat Kcnd1	ACCTGATTCTCACCTACAATCTG	TCTTCCGTTTCATCCTCTCCT
Rat Cacnb4	CACCGTATCCCACAGCAAT	GAGGTCATTAGGCTTCGTCTT
Rat Slc6a1	CCCAGGGTGGCATTATGTCT	GGGTGTGAAAAGGACCAGC
Rat Gabrb2	AAGATGCGCCTGGATGTCAA	ATGCTGGAGGCATCATAGGC
Rat Gabrg1	GTCTTCCTTTTCTCTCCTTCCC	TCATCTTCATCATCTGCTTTATCAATG

References (61-72)